

Manipulation and amplification of the Casimir force through surface fields using helicity

Daniel Dantchev^{1,2}, and Joseph Rudnick¹

¹ *Department of Physics and Astronomy, UCLA, Los Angeles, California 90095-1547, USA,*

² *Institute of Mechanics - BAS, Academic Georgy Bonchev St. building 4, 1113 Sofia, Bulgaria*
(Dated: February 27, 2017)

We present both exact and numerical results for the behavior of the Casimir force in $O(n)$ systems with a finite extension in one direction when the system is subjected to surface fields that induce helicity in the order parameter. We show that for such systems the Casimir force in certain temperature ranges is of the order of L^{-2} , both above and below the critical temperature, T_c , of the bulk system. An example of such a system would be one with chemically modulated bounding surfaces, in which the modulation couples directly to the system's order parameter. We demonstrate that, depending on the parameters of the system, the Casimir force can be either *attractive* or *repulsive*. The exact calculations presented are for the one dimensional XY and Heisenberg models under twisted boundary conditions resulting from finite surface fields that differ in direction by a specified angle and the three dimensional Gaussian model with surface fields in the form of plane waves that are shifted in phase with respect to each other. Additionally, we present exact and numerical results for the mean field version of the three dimensional $O(2)$ model with finite surface fields on the bounding surfaces. We find that all significant results are consistent with the expectations of finite size scaling.

PACS numbers: 64.60.-i, 64.60.Fr, 75.40.-s

I. INTRODUCTION

Casimir forces result from, and provide insight into, the behavior of a medium confined to a restricted space, canonically the region between two plane, parallel surfaces. In the case of the electromagnetic Casimir force, the medium is the vacuum, and the underlying mechanism is the set of quantum zero point or temperature fluctuations of the electromagnetic field. The now widely-investigated critical Casimir force (CCF) results from the fluctuations of an order parameter and more generally the thermodynamics of the medium supporting that order parameter in the vicinity of a critical point. In fact, the free energy of a confined medium can mediate a Casimir force at any temperature provided its excitations are long-range correlated ones. This fact, along with the wide range of options for a mediating substance opens up a range of possibilities for the study and exploitation of the Casimir force arising from a confined medium.

One of the principal influences on the Casimir force is the nature of the bounding surface. With respect to the CCF, published investigations have been focused, almost exclusively, on systems belonging to the Ising universality class. On a basic level, based on the behavior of coupling in the vicinity of the surface, there are three universality classes—extraordinary (or normal), ordinary and surface-bulk (or special), ones [1–3]. Experimental investigations into the influence of surface universality classes on the Casimir force have been reported in [4–10]. Most of them focus on the behavior of colloids in a critical solvent. They probe the dependence of the force between boundaries on temperature, the concentration of the components of the solvent and the relative preference of the surfaces of the colloids for the com-

ponents of the solvent. For example, in [7] the critical thermal noise in a solvent medium consisting of a binary liquid mixture of water and 2,6-lutidine near its lower consolute point is shown to lead to attractive or repulsive forces, depending on the relative adsorption preferences of the colloid and substrate surfaces with respect to the two components of the binary liquid mixture. On the theoretical side, the influence of the surface fields has been studied on the case of two dimensional Ising model via exact calculation [11–14], using the variational formulation due to Mikheev and Fisher [15, 16], with the help of density-matrix renormalization-group numerical method [17–20], via conformal invariance [21, 22], Monte Carlo methods [21], and numerically using bond propagation algorithms [23]. The three dimensional Ising model has been studied with Monte Carlo methods in [24–30], mean-field type calculations [31–36] and renormalized local functional theory [37]. In general, it has been shown that the Casimir force depends on the strength of the surface fields h_1 and h_2 and that it can change sign as the magnitudes of the surface field, the thickness of the films, and the temperature of the system are varied.

For the general case of $O(n)$ systems there is no similarly thorough classification [38]. References [39–47] report on studies of the Casimir force in liquid crystals, and [48–54] describe investigations for ^4He and ^3He – ^4He mixtures. In the case of Helium films, however, it is generally accepted that the boundary conditions are determined, in the region where the liquid behaves as a quantum liquid, by its quantum nature and, thus, cannot be easily influenced by modification of bounding surfaces, in that there are no surface fields that couple to the order parameter in such systems. In that respect liquid crystals seem much more readily adjustable, and in particular more amenable

to the influence of boundary conditions. For example, in Ref. [39] it is shown that director fluctuations in nematics induce long-range interactions between walls, which are attractive with symmetric boundary conditions, but may become repulsive with mixed ones. In smectics such forces are longer ranged than van der Waals ones.

In [41] the authors concluded that in the case of finite surface coupling, the fluctuation-induced forces for nematics are weaker than in the strong anchoring limit. In the example of three-dimensional lattice XY model with nearest neighbor interaction, it has been shown [55] that the Casimir force depends in a continuous way on the parameter α characterizing the so-called twisted boundary conditions when the angle between the vector order parameter at the two boundaries is α where $0 < \alpha \leq \pi$. The effect is essential; depending on α the force can be attractive or repulsive. By varying α and/or the temperature T one can control both the sign and the magnitude of the Casimir force in a reversible way. Furthermore, when $\alpha = \pi$, an additional phase transition, which occurs only in finite systems, has been discovered, associated with the spontaneous symmetry breaking of the direction of rotation of the vector order parameter through the body of the system.

In the current article we show that the strength and the mutual orientation of surface fields—as well as structuring on the surface via chemical or other alternations that can be described in terms of surface fields—lead to interesting and substantial modification in the behavior of the force between the confining surface. Such modification includes the change of the sign of the force, as well as non-monotonic behavior, appearance of multiple minima, of a longitudinal Casimir force, and also an amplification of the force in regions with strong helicity effects. We will demonstrate the above with the example of few models: the one dimensional XY and Heisenberg models, the three dimensional Gaussian model and the three dimension $O(2)$ XY model.

We start with the one-dimensional XY and Heisenberg models.

II. 1D CONTINUUM SYMMETRY MODELS WITH BOUNDARY FIELDS

Here we consider two one-dimensional models with continuous $O(n)$ spin symmetry: XY ($n = 2$) and Heisenberg ($n = 3$) chains of N spins with ferromagnetic interaction J between nearest-neighbor spins, the boundary fields \mathbf{H}_1 and \mathbf{H}_2 of which are at an angle $0 \leq \psi \leq \pi$ with respect to each other. Obviously, such systems do not exhibit spontaneous ordering at non-zero temperatures given their low dimension and the short range nature of the interactions between spins, as has been shown to follow rigorously from the Mermin-Wagner theorem [56]. Nevertheless, they possess an essential singular point at $T = 0$ and will, in that limit, support spontaneous order. We will demonstrate that when the boundary fields

are non-zero the Casimir force, F_{Cas} , of these systems displays very rich and interesting behavior. We also show that near $T = 0$ the force has a scaling behavior and that, depending on the angle between the boundary fields and the value of the temperature scaling variable $x \sim Nk_B T/J$, this force can be *attractive* or *repulsive*. More precisely, we will establish that:

- i) For low temperatures, when $x = \mathcal{O}(1)$ and

$$N \gg J \left(\frac{1}{H_1} + \frac{1}{H_2} \right) \quad (2.1)$$

the leading behavior of the Casimir force can be written in the form

$$\beta F_{\text{Cas}}(T, N, \mathbf{H}_1, \mathbf{H}_2) = N^{-1} X(\psi, x), \quad (2.2)$$

with x a scaling variable and X a universal scaling function. Equation (2.2) implies that, under constraint Eq. (2.1), X_{Cas} depends only on the scaling variable x defined in (2.12) and the angle ψ . The latter parameter effectively describes the boundary conditions on the system. Note that, unlike the Ising model, the boundary conditions depend here *continuously* on one parameter—in our notation ψ .

- ii) When $x \rightarrow 0+$ the scaling function of the Casimir force becomes positive, i.e., the force turns *repulsive* provided that $\psi \neq 0$. In that case $X_{\text{Cas}} \sim x^{-1}$ and, thus, the overall N -dependence of the force is of the order of N^{-2} .
- iii) When $x \gtrsim 1$ the scaling function has a sign that depends on the sign of $\cos(\psi)$: for $0 < |\psi| < \pi/2$ the force will be *attractive*, while for $\pi/2 < |\psi| < \pi$ it will be *repulsive*. For $x \gg 1$ the force decays exponentially to zero.
- iv) For any ψ such that $0 < |\psi| < \pi/2$ the Casimir force *changes from attractive to repulsive* when the temperature decreases from a moderate value to zero for fixed system size, N .
- v) When $\psi = 0$ the force is attractive for *any* value of the scaling variable x .

These 1d models have been studied analytically in the case of free (frequently termed “open” or Dirichlet) and periodic boundary conditions [57–61], but we are not aware of any investigation of them in the presence of boundary fields, which are responsible for the effects of interest in this article.

A. The 1d XY model

We consider a system with the Hamiltonian

$$\mathcal{H} = -J \sum_{i=1}^{N-1} \mathbf{S}_i \cdot \mathbf{S}_{i+1} - \mathbf{H}_1 \cdot \mathbf{S}_1 - \mathbf{H}_N \cdot \mathbf{S}_N \quad (2.3)$$

where \mathbf{S}_i , with $\mathbf{S}_i^2 = 1$ and $\mathbf{S}_i \in \mathbb{Z}^2$, $i = 1, \dots, N$, are N spins arranged along a straight line. The Hamiltonian can be written in the form

$$\mathcal{H} = -J \sum_{i=1}^{N-1} \cos(\varphi_{i+1} - \varphi_i) - H_1 \cos(\psi_1 - \varphi_1) - H_N \cos(\psi_N - \varphi_N), \quad (2.4)$$

where the angles ψ_1, ψ_2 and $\varphi_1, \dots, \varphi_N$ are measured with respect to the line of the chain which is taken to be, say, the x axis. The free energy $-\beta F_N$ of this system is given by

$$\exp(-\beta F_N) = \int_0^{2\pi} \exp(-\beta \mathcal{H}) \prod_{i=1}^N \frac{d\varphi_i}{2\pi}. \quad (2.5)$$

Performing the requisite calculations (see Appendix A)

one obtains

$$\begin{aligned} & \exp(-\beta F_N) \\ &= \sum_{k=-\infty}^{\infty} \exp(ik\psi) I_k(h_1) I_k(K)^{N-1} I_k(h_N) \end{aligned} \quad (2.6)$$

where

$$\psi \equiv (\psi_1 - \psi_N), K \equiv \beta J, h_1 \equiv \beta H_1, h_N \equiv \beta H_N. \quad (2.7)$$

Note that the free energy depends only on the difference in angles, $(\psi_1 - \psi_N)$, and not on ψ_1 and ψ_N separately. For the Casimir force in the system, i.e., for the finite size part of the total force, see Eq. (A8), one then has the *exact* expression

$$\beta F_{\text{Cas}} = \frac{2 \sum_{k=1}^{\infty} \cos[k(\psi_1 - \psi_2)] \log \left[\frac{I_k(K)}{I_0(K)} \right] \frac{I_k(h_1)}{I_0(h_1)} \left(\frac{I_k(K)}{I_0(K)} \right)^{N-1} \frac{I_k(h_N)}{I_0(h_N)}}{1 + 2 \sum_{k=1}^{\infty} \cos[k(\psi_1 - \psi_2)] \frac{I_k(h_1)}{I_0(h_1)} \left(\frac{I_k(K)}{I_0(K)} \right)^{N-1} \frac{I_k(h_N)}{I_0(h_N)}}. \quad (2.8)$$

From here on we will be interested in the behavior of the system in the limit $\beta \gg 1$, i.e., when $T \rightarrow 0$. Obviously, when $\beta \gg 1$ from Eq. (2.7) one has $h_1 \gg 1$, $h_N \gg 1$ and $K \gg 1$, which means that in Eq. (2.6) one uses the large argument asymptote of $I_k(z)$ for $z \gg 1$. We will use the asymptote in the form reported in [62]

$$I_\nu(z) = \frac{e^{z-\nu^2/2z}}{\sqrt{2\pi z}} \left[1 + \frac{1}{8z} + \mathcal{O}\left(\frac{\nu^2}{z^2}\right) \right]. \quad (2.9)$$

Retaining only the first term in the above expansion, one obtains

$$\beta F_{\text{Cas}}(x) = \frac{1}{N_{\text{eff}}} X_{\text{Cas}}(\psi, x, h_{\text{eff}}) \quad (2.10)$$

where

$$X_{\text{Cas}} = -x \frac{\sum_{k=1}^{\infty} k^2 \cos(k\psi) \exp\left[-\frac{1}{2}k^2(h_{\text{eff}}^{-1} + x)\right]}{1 + 2 \sum_{k=1}^{\infty} \cos(k\psi) \exp\left[-\frac{1}{2}k^2(h_{\text{eff}}^{-1} + x)\right]}, \quad (2.11)$$

and

$$x \equiv \frac{N_{\text{eff}}}{K}, \quad h_{\text{eff}}^{-1} = h_1^{-1} + h_2^{-1}, \quad N_{\text{eff}} = N - 1. \quad (2.12)$$

Here, x is the scaled version of the reduced temperature variable, which in systems with a non-zero transition temperature takes the form $x = t^\nu L$, with t the reduced temperature $\propto T - T_c$, L the characteristic size of the finite system and ν the correlation length exponent. Recall that with an effective transition temperature of $T = 0$ and $K \propto 1/T$, the definition in (2.12) is consistent with this definition under the assumption that $\nu = 1$.

Obviously, when Eq. (2.1) is fulfilled one has $x \gg h_{\text{eff}}^{-1}$, and one can safely ignore h_{eff} in Eq. (2.11). Then the behavior of the force is exactly as stated in Eq. (2.2).

The representation of X_{Cas} given by Eq. (2.11) is convenient for all values of x except in the limit $x \ll 1$. For that limit, using the Poisson identity Eq. (A9), one obtains

$$X_{\text{Cas}}(\psi, x, h_{\text{eff}}) = -\frac{x}{2(x + h_{\text{eff}}^{-1})} \quad (2.13)$$

$$+ \frac{x}{2(x + h_{\text{eff}}^{-1})^2} \frac{\sum_{n=-\infty}^{\infty} (2n\pi + \psi)^2 \exp\left[-\frac{(2n\pi + \psi)^2}{2(x + h_{\text{eff}}^{-1})}\right]}{\sum_{n=-\infty}^{\infty} \exp\left[-\frac{(2n\pi + \psi)^2}{2(x + h_{\text{eff}}^{-1})}\right]}.$$

Under the assumption that the constraint (2.1) is fulfilled and given the asymptotic behavior of X_{Cas} from Eqs. (2.11) and (2.13), we derive

$$X_{\text{Cas}}(\psi, x) = \begin{cases} -\frac{1}{2} + \frac{1}{2x}\psi^2 + \dots, & x \rightarrow 0+ \\ -x \cos(\psi) \exp(-x/2), & x \gg 1. \end{cases} \quad (2.14)$$

From Eq. (2.13) one can also derive an expression for the low T behavior of the system that retains the dependence on H_1 and H_2 . The result is

$$\begin{aligned} \beta F_{\text{Cas}} &= -\frac{1}{2} \frac{1}{(J/H_1 + J/H_N + N - 1)} \\ &+ \frac{1}{2} K \frac{(\psi_1 - \psi_N)^2}{(J/H_1 + J/H_N + N - 1)^2}. \end{aligned} \quad (2.15)$$

This result can be also directly derived by realizing that the ground state of the system is a spin wave such that

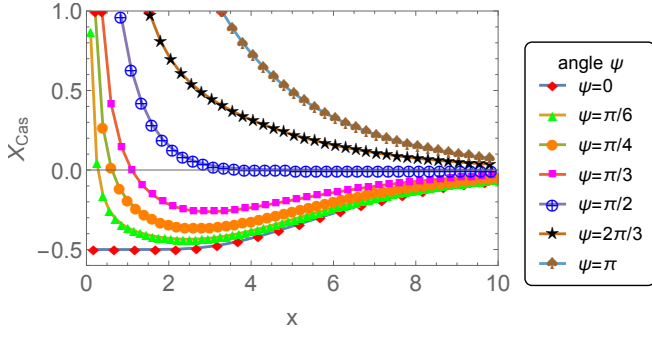


FIG. 1. (Color online) The scaling function X_{Cas} of the XY model as a function of the scaling variable x , see Eq. (2.12), for different values of the phase change ψ .

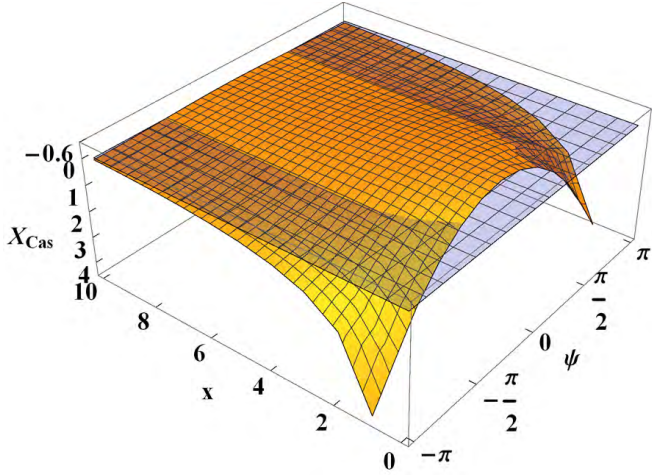


FIG. 2. (Color online) The surface of the scaling function $X_{\text{Cas}}(\psi, x)$ of the XY model as a function of the scaling variables x and ψ . The horizontal plane marks the $X_{\text{Cas}} = 0$ value.

the end spins are twisted with respect to each other at

angle $\psi = \psi_1 - \psi_N$.

Equations (2.11), (2.13), (2.14) and (2.15) confirm the validity of the statements i)-iv) in the first part of this section. For example, Eq. (2.11) demonstrates that when $\psi = 0$ the force is attractive for *any* value of the scaling variable x ; Eq. (2.14) then confirms this behavior for small and large values of the scaling variable x .

The behavior of the scaling function $X_{\text{Cas}}(\psi, x)$ for different values of ψ as a function of the scaling variable x is shown in Fig. 1. Fig. 2 shows a 3D plot of this function for $x \in [0, 10]$ and $\psi \in [-\pi, \pi]$.

B. The 1d Heisenberg model

The Hamiltonian of the system is again given by Eq. (2.3) with the conditions that now the N spins \mathbf{S}_i , $i = 1, \dots, N$, again arranged along a straight line, are three-dimensional vectors $\mathbf{S}_i \in \mathbb{Z}^3$, $i = 1, \dots, N$.

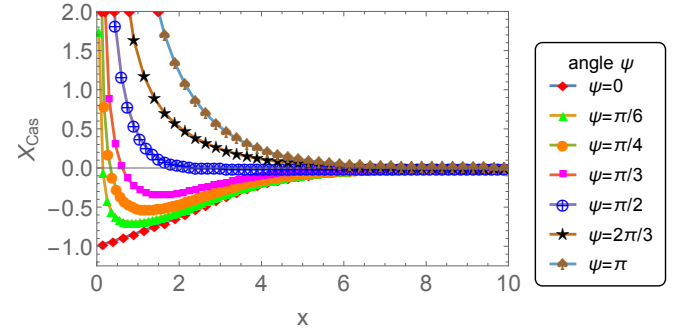


FIG. 3. (Color online) The scaling function X_{Cas} of the Heisenberg model as a function of the scaling variable x , see Eq. (2.21), for different values of the phase change ψ .

As shown in Appendix B the free energy of the system is given by the *exact* expression

$$\begin{aligned} \exp(-\beta F_N) &= \left(\frac{\pi}{2K}\right)^{(N-1)/2} \frac{\pi}{2\sqrt{h_1 h_N}} \sum_{n=0}^{\infty} (2n+1) P_n(\cos \psi_h) I_{n+1/2}(h_1) I_{n+1/2}(h_N) [I_{n+1/2}(K)]^{N-1} \\ &= \frac{\sinh h_1}{h_1} \frac{\sinh h_N}{h_N} \left[\frac{\sinh K}{K}\right]^{N-1} \left\{ 1 + \sum_{n=1}^{\infty} (2n+1) P_n(\cos \psi_h) \frac{I_{n+1/2}(h_1)}{I_{1/2}(h_1)} \frac{I_{n+1/2}(h_N)}{I_{1/2}(h_N)} \left[\frac{I_{n+1/2}(K)}{I_{1/2}(K)}\right]^{N-1} \right\}, \end{aligned} \quad (2.16)$$

where ψ_h is the angle between the vectors \mathbf{H}_1 and \mathbf{H}_N and we have used that $I_{1/2}(x) = \sqrt{2/(\pi x)} \sinh(x)$. Here $I_{n+1/2}(z)$ is the modified Bessel function of the first kind of half-integer index, $P_n(x)$ is the Legendre polynomial of degree n and K , h_1 and h_N are defined in accord with Eq. (2.17).

$$K \equiv \beta J, h_1 \equiv \beta H_1, h_N \equiv \beta H_N. \quad (2.17)$$

When $h_1 \rightarrow 0$ and $h_N \rightarrow 0$ the system considered becomes the one with Dirichlet boundary conditions, a case that was studied by M. E. Fisher in [57]. Taking into account that $I_{n+1/2}(x) = [2^{n+1/2} \Gamma(n+3/2)]^{-1} x^{n+1/2} + \mathcal{O}(x^{5/2+n})$ and that $P_0(x) = 1$, one concludes that only the term with $n = 0$ will contribute to the free energy in

this case. One obtains

$$\begin{aligned} \exp(-\beta F_N) &= \left(\frac{\pi}{2K}\right)^{(N-1)/2} [I_{1/2}(K)]^{N-1} \quad (2.18) \\ &= \left[\frac{\sinh K}{K}\right]^{N-1}. \end{aligned}$$

The last expression is precisely the result derived in [57].

From Eq. (2.16) one can easily derive the corresponding *exact* expression for the Casimir force for the one dimensional Heisenberg model. One has

$$\beta F_{\text{Cas}} = \frac{\sum_{n=1}^{\infty} (2n+1) P_n(\cos \psi_h) \ln \left[\frac{I_{n+1/2}(K)}{I_{1/2}(K)} \right] \frac{I_{n+1/2}(h_1)}{I_{1/2}(h_1)} \frac{I_{n+1/2}(h_N)}{I_{1/2}(h_N)} \left[\frac{I_{n+1/2}(K)}{I_{1/2}(K)} \right]^{N-1}}{1 + \sum_{n=1}^{\infty} (2n+1) P_n(\cos \psi_h) \frac{I_{n+1/2}(h_1)}{I_{1/2}(h_1)} \frac{I_{n+1/2}(h_N)}{I_{1/2}(h_N)} \left[\frac{I_{n+1/2}(K)}{I_{1/2}(K)} \right]^{N-1}}. \quad (2.19)$$

In the limit $T \rightarrow 0$ when $h_1 \gg 1$, $h_N \gg 1$ and $K \gg 1$ from Eq. (2.9) one obtains

$$\beta F_{\text{Cas}}(x) = \frac{1}{N_{\text{eff}}} X_{\text{Cas}}(\psi_h, x, h_{\text{eff}}) \quad (2.20)$$

where the scaling variable x , as well as h_{eff} , are as defined in Eq. (2.12) while the scaling function X_{Cas} is

$$X_{\text{Cas}}(\psi_h, x, h_{\text{eff}}) = -\frac{1}{2} x \frac{\sum_{n=1}^{\infty} n(n+1)(2n+1) P_n(\cos \psi_h) \exp \left[-\frac{1}{2} n(n+1) (x + h_{\text{eff}}^{-1}) \right]}{1 + \sum_{n=1}^{\infty} (2n+1) P_n(\cos \psi_h) \exp \left[-\frac{1}{2} n(n+1) (x + h_{\text{eff}}^{-1}) \right]}. \quad (2.21)$$

As in the case of the XY model, when Eq. (2.1) is fulfilled one can ignore h_{eff} in the above expression. If not stated otherwise we will always suppose this to be the case. Then the scaling function X_{Cas} depends only on the scaling variable x and the angle ψ_h that parametrizes the boundary conditions on the system, exactly as set forth in Eq. (2.2). The representation of X_{Cas} given by

Eq. (2.21) is applicable for all values of x except in the limit $x \ll 1$. Keeping in mind that $P_1(\cos \psi_h) = \cos \psi_h$, and in light of the fast decay off the terms in the sums in Eq. (2.22), it is clear that for those very small values of x the sign of the force will be determined by the sign of $\cos \psi_h$. For the leading behavior of the Casimir force when $x \ll 1$ one obtains

$$X_{\text{Cas}}(\psi_h, x, h_{\text{eff}}) = -1 + \frac{h_{\text{eff}}^{-1}}{h_{\text{eff}}^{-1} + x} + \frac{x(1 - \cos \psi_h)}{(h_{\text{eff}}^{-1} + x)^2} + x \frac{\coth \left(\frac{1}{h_{\text{eff}}^{-1} + x} \right) - 1}{(h_{\text{eff}}^{-1} + x)^2}, \quad (2.22)$$

which follows from Eq. (B16). One can also derive the first three terms in that expansion by considering the N dependence of the ground energy of the 1d Heisenberg model, assuming it to be in the form of a spin wave. Explicitly, for the behavior of the Casimir force for $T \rightarrow 0$ from Eq. (2.22) one obtains

$$\begin{aligned} \beta F_{\text{Cas}} &= -\frac{1}{(J/H_1 + J/H_N + N - 1)} \\ &+ K \frac{1 - \cos \psi_h}{(J/H_1 + J/H_N + N - 1)^2}. \quad (2.23) \end{aligned}$$

The behavior of the scaling function $X_{\text{Cas}}(\psi, x)$ for different values of ψ as a function of the scaling variable x is shown in Fig. 3 while Fig. 4 shows a 3D plot of this function for $x \in [0, 10]$ and $\psi \in [-\pi, \pi]$. Thus, for the

overall behavior of the Casimir force as a function of ψ_h one arrives at the same set of conclusions for the Heisenberg model as for the XY model as a function of ψ , as summarized in statements i)-v).

III. THE 3D GAUSSIAN MODEL

Here, we focus on a system with scalar spins. This means that, strictly speaking, there is no helicity. However, the surface fields that influence the order parameter will have sinusoidal variation along the film boundaries, conforming to the behavior of the individual components of a field that induces helical order in a multi-component system. We therefore expect that the results to be de-

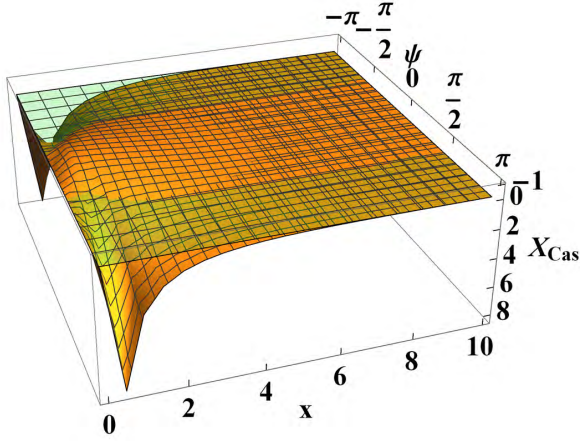


FIG. 4. (Color online) The surface of the scaling function $X_{\text{Cas}}(\psi, x)$ of the Heisenberg model as a function of the scaling variables x and ψ . The horizontal plane marks the $X_{\text{Cas}} = 0$ value.

$$\begin{aligned}
 -\beta\mathcal{H} = & \sum_{x=1}^M \sum_{y=1}^N \left\{ K^{\parallel} \sum_{z=1}^L S_{x,y,z} (S_{x+1,y,z} + S_{x,y+1,z}) + K^{\perp} \sum_{z=1}^{L-1} S_{x,y,z} S_{x,y,z+1} + h_1 S_{x,y,1} \cos(k_x x + k_y y) \right. \\
 & \left. + h_L S_{x,y,L} \cos(k_x (x + \Delta_x) + k_y (y + \Delta_y)) - s \sum_{z=1}^L S_{x,y,z}^2 \right\} \quad (3.1)
 \end{aligned}$$

which describes a system with short-ranged nearest neighbor interactions possessing chemically modulated bounding surfaces situated at $z = 1$ and $z = L$. Here $h_1 = \beta H_1$ and $h_L = \beta H_L$ are the external fields acting only on the boundaries of the system. In the specific example considered the modulation depends on the coordinates x and y in a wave-like way specified by the applied surface fields $h_1 \cos(k_x x + k_y y) \equiv h_1 \cos(\mathbf{k} \cdot \mathbf{r})$ and $h_L \cos[k_x (x + \Delta_x) + k_y (y + \Delta_y)] \equiv h_L \cos(\mathbf{k} \cdot (\mathbf{r} + \mathbf{\Delta}))$, the phases of which are thus shifted with respect to each other by Δ_x in x direction and by Δ_y in y direction. Here $\mathbf{r} = (x, y)$, $\mathbf{k} = (k_x, k_y)$ and $\mathbf{\Delta} = (\Delta_x, \Delta_y)$. Periodic boundary conditions are applied along the x and y axes, while missing neighbor (Dirichlet) boundary conditions are imposed in the z direction. These boundary conditions are expressed as follows:

$$S_{1,y,z} = S_{M+1,y,z}, \quad S_{x,1,z} = S_{x,N+1,z} \quad (3.2)$$

and

$$S_{x,y,0} = 0 \quad \text{and} \quad S_{x,y,L+1} = 0. \quad (3.3)$$

Given those the boundary conditions, the Hamiltonian

rived and discussed in this section will be germane to corresponding behavior in such a system. We consider a planar discrete system containing L two-dimensional layers with a Hamiltonian

in Eq. (3.1) can be rewritten in the form

$$\begin{aligned}
 -\beta\mathcal{H} = & \sum_{x=1}^M \sum_{y=1}^N \sum_{z=1}^L S_{x,y,z} \left\{ K^{\parallel} (S_{x+1,y,z} + S_{x,y+1,z}) \right. \\
 & + K^{\perp} S_{x,y,z+1} + \delta_{1,z} h_1 \cos[\mathbf{k} \cdot \mathbf{r}] \\
 & \left. + \delta_{L,z} h_L \cos[\mathbf{k} \cdot (\mathbf{r} + \mathbf{\Delta})] - s S_{x,y,z} \right\}. \quad (3.4)
 \end{aligned}$$

Since we will be considering the limit $M, N \rightarrow \infty$ we can always take the wave vector components k_x and k_y to coincide with $(2\pi p)/M$ and $(2\pi q)/N$ for some $p = 1, \dots, M$ and $q = 1, \dots, N$, respectively. In Eqs. (3.1) and (3.4) one has

$$K^{\parallel} = \beta J^{\parallel}, \quad \text{and} \quad K^{\perp} = \beta J^{\perp}, \quad (3.5)$$

where J^{\parallel} and J^{\perp} are the strengths of the coupling constants along and perpendicular to the L layers of the system. The parameter $s > 0$ on the right hand side of (3.4) is subjected to the constraint that it has a value that ensures the existence of the partition function of the system. It is easy to check that $2K^{\parallel} + K^{\perp} - s \equiv \beta(2J^{\parallel} + J^{\perp}) - s = 0$ determines the critical temperature β_c of the bulk model, i.e., one has

$$\beta_c = s / (2J^{\parallel} + J^{\perp}). \quad (3.6)$$

For the model defined above the Casimir force acting on the bounding planes at $z = 1$ and $z = L$ has both orthogonal, $\beta F_{\text{Cas}}^{(\perp)}$, and lateral, $\beta F_{\text{Cas}}^{(\parallel, \alpha)}$, $\alpha = x$ or $\alpha = y$, components, which can be written in the form

$$\beta F_{\text{Cas}}^{(\cdots)} = L^{-3} \left(\frac{J^\perp}{J^\parallel} \right) X_{\text{Cas}}^{(\cdots)}(x_t, x_k, x_1, x_L), \quad (3.7)$$

where (\cdots) stands for either (\perp) or (\parallel, α) , with $\alpha = x$ or $\alpha = y$. Here

$$x_1 = \sqrt{LK^\parallel} \frac{h_1}{K^\perp}, \quad x_L = \sqrt{LK^\parallel} \frac{h_L}{K^\perp}, \quad (3.8)$$

are the field-dependent scaling variables, x_t is the temperature-dependent one with

$$x_t = L \sqrt{2 \left(\frac{\beta_c}{\beta} - 1 \right) \left[2 \frac{J^\parallel}{J^\perp} + 1 \right]}, \quad x_k = \sqrt{\frac{J^\parallel}{J^\perp}} Lk, \quad (3.9)$$

with $k = \sqrt{k_x^2 + k_y^2}$ is the scaling variable related to the surface modulation. When $h_1 = \mathcal{O}(1)$ and $h_L = \mathcal{O}(1)$ we will see that $F_{\text{Cas}}^{(\cdots)}$ has a *field dependent contribution* which, in this regime, will provide the *leading* contribution to the force of the order of L^{-2} .

The Hamiltonian (3.4) can be easily diagonalized in a standard way—see Appendix C. The resulting free energy of the system, F , is

$$F = \Delta F_0 + \Delta F_h, \quad (3.10)$$

where

$$\begin{aligned} -\beta \Delta F_0 &= \frac{1}{2} MNL \ln \pi \\ -\frac{1}{2} \sum_{l=1}^L \sum_{m=1}^M \sum_{n=1}^N \ln \left\{ s - K^\parallel \left[\cos \left(\frac{2\pi m}{M} \right) + \cos \left(\frac{2\pi n}{N} \right) \right] \right. \\ &\quad \left. - K^\perp \cos \left(\frac{\pi l}{L+1} \right) \right\} \end{aligned} \quad (3.11)$$

is the field independent part of the free energy and ΔF_h , the field dependent contribution, is

i) when either $p \neq M$ or $q \neq N$:

$$\begin{aligned} -\beta \Delta F_h &= \frac{MN}{8(L+1)} \times \\ &\sum_{l=1}^L \frac{\sin^2 \left(\frac{\pi l}{L+1} \right) [h_1^2 + h_L^2 - 2h_L h_1 (-1)^l \cos(\mathbf{k} \cdot \mathbf{\Delta})]}{s - K^\parallel \left[\cos \left(\frac{2\pi p}{M} \right) + \cos \left(\frac{2\pi q}{N} \right) \right] - K^\perp \cos \left(\frac{\pi l}{L+1} \right)}, \end{aligned} \quad (3.12)$$

where $\mathbf{k} = (k_x = 2\pi p/M, k_y = 2\pi q/N)$, and $\mathbf{\Delta} = (\Delta_x, \Delta_y)$, and

ii) when $p = M$ and $q = N$:

$$\begin{aligned} -\beta \Delta F_h &= \frac{MN}{2(L+1)} \times \\ &\sum_{l=1}^L \frac{\sin^2 \left(\frac{\pi l}{L+1} \right) [h_1 - h_L (-1)^l \cos(2\pi(\Delta_x + \Delta_y))]^2}{s - 2K^\parallel - K^\perp \cos \left(\frac{\pi l}{L+1} \right)}. \end{aligned} \quad (3.13)$$

Note that there is a fundamental difference between the sub-cases in Eqs. (3.12) and (3.13); while in the first sub-case *i*) the average field applied on the surfaces is zero when specially averaged, in the second sub-case *ii*) it is a constant. In the last sub-case one can think of h_L as a constant field acting on the second surface being twisted in direction with respect to the constant field h_1 applied to the first one with a twist governed by Δ_x and Δ_y .

Obviously

$$\begin{aligned} s - K^\parallel \left[\cos \left(\frac{2\pi m}{M} \right) + \cos \left(\frac{2\pi n}{N} \right) \right] - K^\perp \cos \left(\frac{\pi k}{L+1} \right) \\ = (\beta_c/\beta - 1) [2K^\parallel + K^\perp] + K^\perp \left[1 - \cos \left(\frac{\pi k}{L+1} \right) \right] \\ + K^\parallel \left[2 - \cos \left(\frac{2\pi m}{M} \right) - \cos \left(\frac{2\pi n}{N} \right) \right] > 0 \end{aligned} \quad (3.14)$$

for $\beta < \beta_c$. The above implies that the statistical sum of the infinite system exists for all $\beta < \beta_c$. The statistical sum of the finite system exists, however, under the less demanding constraint that

$$(\beta_c/\beta - 1) [2J^\parallel + J^\perp] + J^\perp \left[1 - \cos \left(\frac{\pi}{L+1} \right) \right] > 0. \quad (3.15)$$

In the remainder we will assume that the constraint given by Eq. (3.15) is fulfilled for all temperatures considered here.

For the contribution of the field-independent term to the transverse Casimir force

$$\beta \Delta F_{\text{Cas}}^{(0, \perp)} = -\frac{\partial}{\partial L} (\beta \Delta f_0), \quad (3.16)$$

with

$$\Delta f_0 = \lim_{M, N \rightarrow \infty} \frac{\Delta F_0}{MN}, \quad (3.17)$$

it is demonstrated in Appendix C that

$$\beta \Delta F_{\text{Cas}}^{(0, \perp)} = -\frac{1}{2} \int_{-\pi}^{\pi} \int_{-\pi}^{\pi} \delta [\coth((1+L)\delta) - 1] \frac{d\theta_1 d\theta_2}{(2\pi)^2}, \quad (3.18)$$

where $\delta = \delta(\theta_1, \theta_2 | \beta_c/\beta, J^\parallel/J^\perp)$ is given by the expression

$$\begin{aligned} \cosh \delta &= 1 + \left(\frac{\beta_c}{\beta} - 1 \right) \left(1 + 2 \frac{J^\parallel}{J^\perp} \right) \\ &\quad + \frac{J^\parallel}{J^\perp} (2 - \cos \theta_1 - \cos \theta_2). \end{aligned} \quad (3.19)$$

The result in Eq. (3.18) is an *exact* expression for $\beta \Delta F_{\text{Cas}}^{(0, \perp)}$; no approximations have been made. Since $\coth(x) > 1$ for $x > 0$ one immediately concludes that $\Delta F_{\text{Cas}}^{(0, \perp)} < 0$, i.e., it is an *attractive* force, for *all* values of L . In order to obtain scaling and, thus, the scaling form of $\Delta F_{\text{Cas}}^{(0, \perp)}$ we have to consider the regime $L \gg 1$. Obviously, then Casimir force will be exponentially small

if δ is finite. For the scaling behavior of the force—see Appendix C—one obtains

$$\beta \Delta F_{\text{Cas}}^{(0,\perp)} = L^{-3} \left(\frac{J^\perp}{J^\parallel} \right) X_{\text{Cas}}^{(0,\perp)}(x_t) \quad (3.20)$$

where $X_{\text{Cas}}^{(0,\perp)}(x_t)$ is the universal scaling function

$$X_{\text{Cas}}^{(0,\perp)}(x_t) = -\frac{1}{8\pi} \left\{ \text{Li}_3(e^{-2x_t}) + 2x_t \text{Li}_2(e^{-2x_t}) - 2x_t^2 \ln(1 - e^{-2x_t}) \right\}. \quad (3.21)$$

and the scaling variable x_t is

$$x_t = L \sqrt{2 \left(\frac{\beta_c}{\beta} - 1 \right) \left(1 + 2 \frac{J^\parallel}{J^\perp} \right)}, \quad (3.22)$$

in accord with Eq. (C34). It is easy to show that $X_{\text{Cas}}^{(0,\perp)}(x_t)$ is a *monotonically increasing* function of x_t . The behavior of $X_{\text{Cas}}^{(0,\perp)}(x_t)$ is visualized in Fig. 5

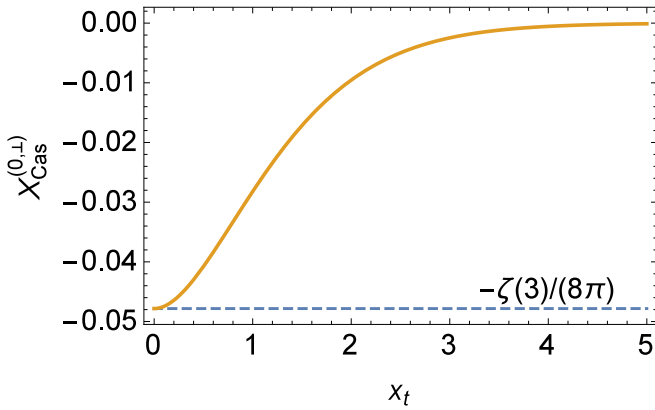


FIG. 5. (Color online) The scaling function $X_{\text{Cas}}^{(0,\perp)}(x_t)$ as a function of the temperature dependent scaling variable x_t . The horizontal line marks the Casimir amplitude $X_{\text{Cas}}^{(0,\perp)}(0) = -\zeta(3)/(8\pi)$.

At the critical point one has $x_t = 0$ and then one immediately obtains the well known Casimir amplitude for the Gaussian model under Dirichlet boundary condition

$$X_{\text{Cas}}^{(0,\perp)}(x_t = 0) = -\frac{\zeta(3)}{8\pi}. \quad (3.23)$$

It is easy to show that

$$X_{\text{Cas}}^{(0,\perp)} \simeq \begin{cases} -\frac{1}{8\pi} \exp(-2x_t) [1 + 2x_t(1 + x_t)], & x_t \gg 1 \\ -\frac{1}{8\pi} \zeta(3) + \frac{1}{48\pi} x_t^2 (6 - 4x_t + x_t^2), & x_t \rightarrow 0. \end{cases} \quad (3.24)$$

For the field component of the transverse Casimir force

$$\beta \Delta F_{\text{Cas}}^{(h,\perp)} = -\frac{\partial}{\partial L} (\beta \Delta f_h) \quad (3.25)$$

where

$$\Delta f_h = \lim_{M,N \rightarrow \infty} \frac{\Delta F_h}{MN} \quad (3.26)$$

one derives, see Eqs. (C22) and (C23) in Appendix C:

i) if $p \neq M$ or $q \neq N$:

$$\begin{aligned} \beta \Delta F_{\text{Cas}}^{(h,\perp)} &= \frac{\lambda \sinh(\lambda)}{32K^\perp} \\ &\times \left\{ [h_1^2 + h_L^2 - 2h_L h_1 \cos(\mathbf{k} \cdot \mathbf{\Delta})]^2 \text{csch}^2 \left[\frac{1+L}{2} \lambda \right] \right. \\ &\quad \left. - [h_1^2 + h_L^2 + 2h_L h_1 \cos(\mathbf{k} \cdot \mathbf{\Delta})]^2 \text{sech}^2 \left[\frac{1+L}{2} \lambda \right] \right\}. \end{aligned} \quad (3.27)$$

and

ii) if $p = M$ and $q = N$

$$\begin{aligned} \beta \Delta F_{\text{Cas}}^{(h,\perp)} &= \frac{\lambda \sinh(\lambda)}{32K^\perp} \\ &\times \left\{ [h_1 - h_L \cos 2\pi(\Delta_x + \Delta_y)]^2 \text{csch}^2 \left[\frac{1+L}{2} \lambda \right] \right. \\ &\quad \left. - [h_1 + h_L \cos 2\pi(\Delta_x + \Delta_y)]^2 \text{sech}^2 \left[\frac{1+L}{2} \lambda \right] \right\}. \end{aligned} \quad (3.28)$$

Here we have introduced the helpful notation

$$\cosh \lambda = \Lambda \quad (3.29)$$

for the case when $\Lambda \geq 1$ and

$$\cos \lambda = \Lambda \quad (3.30)$$

in the opposite case when $\Lambda \leq 1$. Note that

- when $h_1 = \mathcal{O}(1)$, $h_L = \mathcal{O}(1)$ and

$$w = L\lambda/2 \quad (3.31)$$

is such that $w = \mathcal{O}(1)$, the Casimir force is of the order of $\mathcal{O}(L^{-2})$ despite the fact that the system is at a temperature *above* the bulk critical one.

- If h_1 and h_L are such that the field-dependent scaling variables $x_1 = \mathcal{O}(1)$ and $x_L = \mathcal{O}(1)$, see Eq. (3.8), then, in terms of w , the Casimir force $\beta \Delta F_{\text{Cas}}^{(h,\perp)}$ reads

$$\beta \Delta F_{\text{Cas}}^{(h,\perp)} = L^{-3} \left(\frac{J^\perp}{J^\parallel} \right) X_{\text{Cas}}^{(h,\perp)}(w, x_1, x_L) \quad (3.32)$$

where the scaling function $X_{\text{Cas}}^{(h,\perp)}(w, x_1, x_L)$ is

i) if $p \neq M$ or $q \neq N$:

$$\begin{aligned} X_{\text{Cas}}^{(h,\perp)}(w, x_1, x_L) &= \frac{1}{8} w^2 \\ &\times \left\{ [x_1^2 + x_L^2 - 2x_1 x_L \cos(\mathbf{k} \cdot \mathbf{\Delta})] \text{csch}^2 w \right. \\ &\quad \left. - [x_1^2 + x_L^2 + 2x_1 x_L \cos(\mathbf{k} \cdot \mathbf{\Delta})] \text{sech}^2 w \right\}, \end{aligned} \quad (3.33)$$

and

ii) if $p = M$ and $q = N$

$$X_{\text{Cas}}^{(h,\perp)}(w, x_1, x_L) = \frac{1}{8}w^2 \quad (3.34)$$

$$\times \left\{ [x_1 - x_L \cos 2\pi(\Delta_x + \Delta_y)]^2 \text{csch}^2 w \right. \\ \left. - [x_1 + x_L \cos 2\pi(\Delta_x + \Delta_y)]^2 \text{sech}^2 w \right\}.$$

The latter expression implies that in the regime considered here the field-dependent part of the force is of order of L^{-3} , as it is the field-independent part of it.

The asymptotic behavior of $\Delta F_{\text{Cas}}^{(h,\perp)}$ for $w \gg 1$ can be easily obtained from Eqs. (C24) and (C25). The result is

$$\beta \Delta F_{\text{Cas}}^{(h,\perp)} \simeq -\frac{2w^2}{K^\perp L^2} e^{-2w} h_1 h_L \\ \times \begin{cases} \cos(\mathbf{k} \cdot \mathbf{\Delta}), & p \neq M \text{ or } q \neq N, \\ \cos 2\pi(\Delta_x + \Delta_y), & p = M, q = N. \end{cases} \quad (3.35)$$

which implies that in this limit the transverse component of the force is exponentially small in L and attractive or repulsive depending on the product $h_1 h_L \cos[\mathbf{k} \cdot \mathbf{\Delta}]$ or $h_1 h_L \cos 2\pi(\Delta_x + \Delta_y)$.

For the field contribution to the longitudinal component of the Casimir force along the α axis, where $\alpha = x, y$, one has

$$\beta \Delta F_{\text{Cas}}^{(h,\alpha)}(L) = -\frac{\partial}{\partial \Delta_\alpha} \Delta f_h. \quad (3.36)$$

Thus, from Eqs. (C22) and (C23) one derives

i) if $p \neq M$ or $q \neq N$:

$$\beta \Delta F_{\text{Cas}}^{(h,\alpha)}(L) = -\frac{h_1 h_L}{4K^\perp} k_\alpha \sin(\mathbf{k} \cdot \mathbf{\Delta}) \frac{\sinh(\lambda)}{\sinh[\lambda(L+1)]} \quad (3.37)$$

and

ii) if $p = M$ and $q = N$

$$\beta \Delta F_{\text{Cas}}^{(h,\alpha)}(L) = -\frac{\pi \sin[2\pi(\Delta_x + \Delta_y)]}{2K^\perp} h_L \\ \times \left\{ h_1 \frac{\sinh(\lambda)}{\sinh[(L+1)\lambda]} \right. \\ \left. + h_L \cos[2\pi(\Delta_x + \Delta_y)] \left[\Lambda - \frac{\sinh(\lambda)}{\tanh(L+1)\lambda} \right] \right\}. \quad (3.38)$$

When $L\lambda \gg 1$ the above simplifies to

i) if $p \neq M$ or $q \neq N$:

$$\beta \Delta F_{\text{Cas}}^{(h,\alpha)}(L) \simeq -\frac{k_\alpha}{2K^\perp} \sinh[\lambda] e^{-(L+1)\lambda} h_1 h_L \sin(\mathbf{k} \cdot \mathbf{\Delta}) \quad (3.39)$$

and

ii) if $p = M$ and $q = N$

$$\beta \Delta F_{\text{Cas}}^{(h,\alpha)}(L) \simeq \\ -\frac{\pi h_L^2}{4K^\perp} \sin[4\pi(\Delta_x + \Delta_y)] \{ \Lambda - \sinh[\lambda] \} \\ -\frac{\pi}{K^\perp} \sinh[\lambda] e^{-(L+1)\lambda} h_1 h_L \sin[2\pi(\Delta_x + \Delta_y)]. \quad (3.40)$$

Note that in the first sub-case the $L \gg 1$ limit of the lateral force is zero, in the second sub-case, when the average value of the external field on the upper surface is not zero the lateral force tends to a finite, well defined limit which is proportional to the surface area of the system. Obviously, this force has the meaning of a local purely surface force.

Subtracting from $\Delta F_{\text{Cas}}^{(h,\alpha)}$ its L -independent part we obtain the lateral force that will act on the upper surface due to the presence of the lower one if we act in lateral direction on the upper one. In the case $p = M$ and $q = N$ one obtains

$$\beta \delta F_{\text{Cas}}^{(h,\alpha)}(L) \equiv \beta \left[\Delta F_{\text{Cas}}^{(h,\alpha)}(L) - \lim_{L \rightarrow \infty} \Delta F_{\text{Cas}}^{(h,\alpha)}(L) \right] \\ = -\frac{\pi h_L}{2K^\perp} \sin[2\pi(\Delta_x + \Delta_y)] \sinh(\lambda) \left\{ h_1 / \sinh[(L+1)\lambda] \right. \\ \left. + h_L \cos[2\pi(\Delta_x + \Delta_y)] [1 - \coth(L+1)\lambda] \right\}. \quad (3.41)$$

In the other sub-case when $p \neq M$ or $q \neq N$ one has that $\beta \delta F_{\text{Cas}}^{(h,\alpha)}(L) \equiv \beta \Delta F_{\text{Cas}}^{(h,\alpha)}(L)$.

In scaling variables for $\beta \delta F_{\text{Cas}}^{(h,\alpha)}(L)$ one has

$$\beta \delta F_{\text{Cas}}^{(h,\alpha)}(L) = L^{-3} \left(\frac{J^\perp}{J^\parallel} \right) X_{\text{Cas}}^{(h,\alpha)}(w, x_1, x_L), \quad (3.42)$$

where

i) if $p \neq M$ or $q \neq N$:

$$X_{\text{Cas}}^{(h,\alpha)} = -\pi x_1 x_L p_\alpha \sin(\mathbf{k} \cdot \mathbf{\Delta}) \frac{\omega}{\sinh[2\omega]}, \quad (3.43)$$

where $p_\alpha = p$ for $\alpha = x$, and $p_\alpha = q$ for $\alpha = y$.

ii) if $p = M$ and $q = N$:

$$X_{\text{Cas}}^{(h,\alpha)} = -\pi x_L \omega \sin[2\pi(\Delta_x + \Delta_y)] \\ \times \left\{ x_1 / \sinh[2\omega] + x_L \cos[2\pi(\Delta_x + \Delta_y)] [1 - \coth 2\omega] \right\}. \quad (3.44)$$

Eq. (3.42) implies that in the scaling regime the longitudinal Casimir force is of the same order of magnitude as the orthogonal component of the force.

Let us now clarify the physical meaning of the regimes $\omega = \mathcal{O}(1)$ and $\omega \gg 1$ in terms of the temperature T . Taking into account Eq. (C9) one has

$$\Lambda = 1 + \left(\frac{\beta_c}{\beta} - 1 \right) \left[2 \frac{J^\parallel}{J^\perp} + 1 \right] + 2 \frac{J^\parallel}{J^\perp} \left[\sin^2 \frac{k_x}{2} + \sin^2 \frac{k_y}{2} \right], \quad (3.45)$$

where $k_x = 2\pi p/M$, $k_y = 2\pi q/N$, as well as all the other terms in the sum determining Λ are dimensionless. We again have to consider two sub-cases:

i) if $p \neq M$ or $q \neq N$.

In this case, in order to have λ small, one needs to have $\beta/\beta_c \rightarrow 1$, and $k_\alpha \rightarrow 0$, $\alpha = x, y$. Under this conditions one has

$$\lambda \simeq \sqrt{2 \left(\frac{\beta_c}{\beta} - 1 \right) \left[2 \frac{J^\parallel}{J^\perp} + 1 \right] + \frac{J^\parallel}{J^\perp} [k_x^2 + k_y^2]}. \quad (3.46)$$

Then

$$\omega = \frac{1}{2} \sqrt{x_t^2 + x_k^2}, \quad (3.47)$$

where x_t and x_k are defined in Eq. (3.9). From Eq. (3.47) it is clear that in order to have $\omega = \mathcal{O}(1)$ one needs to have simultaneously $x_t = \mathcal{O}(1)$ and $x_k = \mathcal{O}(1)$. Taking into account that $\nu = 1/2$ for the Gaussian model, one has that x_t^2 is in its expected form $a_t t L^{1/\nu}$, with $t = (T - T_c)/T_c$. The condition $x_k = \mathcal{O}(1)$ implies that in order to encounter the regime $\omega = \mathcal{O}(1)$ one needs to have a modulation with a wave vector $k \lesssim L^{-1}$ which includes, e.g., the $k = 0$ case. If $x_k \gg 1$ one will have, even at the critical point $\beta = \beta_c$ that $\omega \gg 1$ and, according to Eq. (3.35), that the field contributions into the Casimir force will be exponentially small then.

ii) if $p = M$ and $q = N$.

As it is clear from Eq. (3.45), this sub-case reduces to the previously considered one with $k_x = k_y = 0$. The last implies that, then, $\omega = x_t/2$.

When $\omega = \mathcal{O}(1)$, from Eqs. (3.27) and (3.28) with $h_1 = \mathcal{O}(1)$ and $h_L = \mathcal{O}(1)$ one has that $\Delta F_{\text{Cas}}^{(h,\perp)} = \mathcal{O}(L^{-2})$, i.e., the longitudinal force in this case is in an order of magnitude *larger* in L than the usual transverse Casimir force, which is of the order of $\mathcal{O}(L^{-3})$.

The behavior of the function $X_{\text{Cas}}^{(h,\perp)}(w, x_1, x_L)$ is visualized in Fig. 6 if i) $p \neq M$ or $q \neq N$ and in Fig. 7 if ii) $p = M$ and $q = N$.

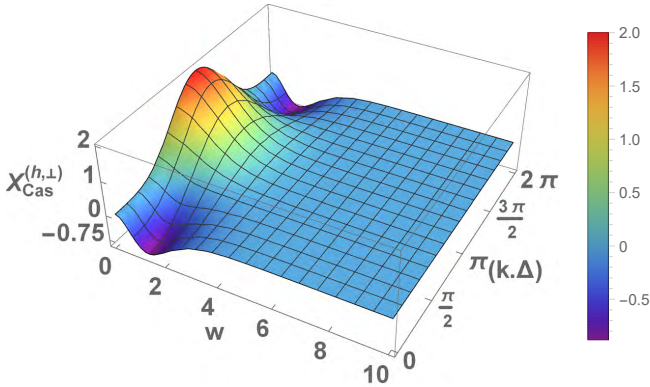


FIG. 6. (Color online) The scaling function $X_{\text{Cas}}^{(h,\perp)}(w, x_1, x_L)$, see Eq. (3.33), as a function of $w \in (0, 10]$ and $(\mathbf{k}, \Delta) \in [0, 2\pi]$ for $x_1 = x_L = 1$. As we see, $X_{\text{Cas}}^{(h,\perp)}(w, x_1, x_L)$ can be both positive and negative, depending on the values of its arguments.

We observe, inspecting the legends, that the maximal values of the function $X_{\text{Cas}}^{(h,\perp)}(w, x_1, x_L)$ are in this case smaller than in previous case shown in Fig. 6.

Let us turn now to the behavior of the total orthogonal Casimir force $F_{\text{Cas}}^{(\perp)}$. From Eqs. (3.10), (3.16), (3.17), (3.20), (3.25) and (3.32) one has

$$F_{\text{Cas}}^{(\perp)} \equiv \Delta F_{\text{Cas}}^{(0,\perp)} + \Delta F_{\text{Cas}}^{(h,\perp)} \quad (3.48)$$

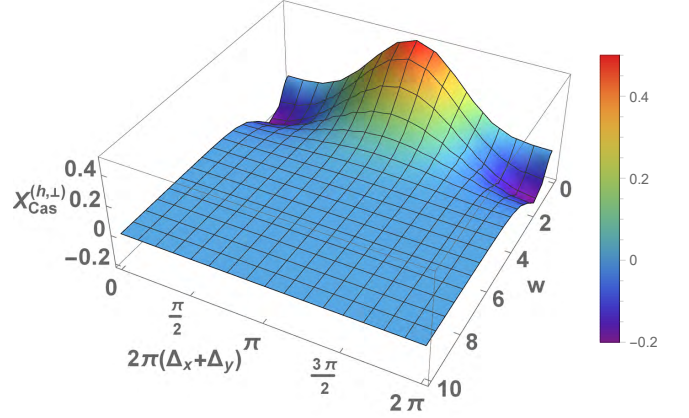


FIG. 7. (Color online) The scaling function $X_{\text{Cas}}^{(h,\perp)}(w, x_1, x_L)$, see Eq. (3.34), as a function of $w \in (0, 10]$ and $\Delta_x + \Delta_y \in [0, 1]$ for $x_1 = x_L = 1$. As we see, also in this case $X_{\text{Cas}}^{(h,\perp)}(w, x_1, x_L)$ can be both positive and negative, depending on the values of its arguments. Let us remind that in this sub-case $\omega = x_t/2$.

and

$$\beta F_{\text{Cas}}^{(\perp)} = L^{-3} \left(\frac{J^\perp}{J^\parallel} \right) X_{\text{Cas}}^{(\perp)}(x_t, x_k, x_1, x_L). \quad (3.49)$$

The behavior of the scaling function of the total orthogonal Casimir force $X_{\text{Cas}}^{(\perp)}(x_t, x_k, x_1, x_L)$ is depicted in Figs. 8 - 10 for the case when i) $p \neq M$ or $q \neq N$ and in the Figs. 11 for the case ii) $p = M$ and $q = N$ with $x_k = 0$. Let us note that in the case i) the function $X_{\text{Cas}}^{(\perp)}$ is symmetric about x_1 and x_L , while in the case ii) that is not so. The last implies that when $x_1 \neq x_L$ in the case ii) we have to consider separately the sub-case $x_1 \gg x_L$ and $x_1 \ll x_L$.

Figs. 8 and 11 show the behavior of the force for equal values of the field scaling variables $x_1 = x_L$. When they are not equal this behavior is visualized in Figs. 9 and 10 for the case i) and in Figs. 12, 13 and 14 for the case ii). Figs. 9 and 12 represent the situation when $x_1 \gg x_L$, namely $x_1 = 10x_L$, while Figs. 10 and 14 represent the results for the case when $x_1 = -x_L = 1$.

The comparison of these figures with Figs. (6) and (7) shows, as it might be expected from the data presented in Fig. (5), that the contribution of $X_{\text{Cas}}^{(0,\perp)}(x_t)$ to the overall behavior of the force is quite small, at least in the depicted cases.

Let us now consider the behavior of the longitudinal Casimir force. We first note that it does not have a contribution that is field-independent. Thus, the scaling function, which characterizes this force, is given by Eq. (3.43) and Eq. (3.44). Because of the term $\sin(\mathbf{k}, \Delta)$, multiplying the expression for the force in the first case, and to $\sin[2\pi(\Delta_x + \Delta_y)]$, in the second case, the scaling function

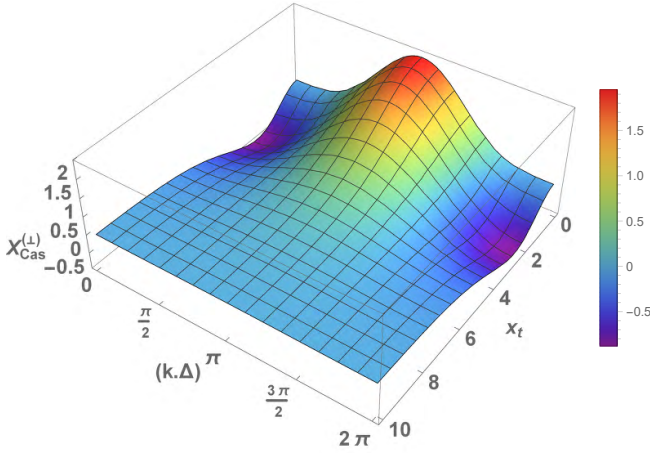


FIG. 8. (Color online) The scaling function $X_{\text{Cas}}^{(\perp)}(x_t, x_k, x_1, x_L)$ as a function of $x_t \in (0, 10]$ and $\mathbf{k} \cdot \Delta \in [0, 2\pi]$ for $x_k = 0.1$, $x_1 = x_L = 1$. As we see, $X_{\text{Cas}}^{(\perp)}$ can be both positive and negative, depending on the values of its arguments.

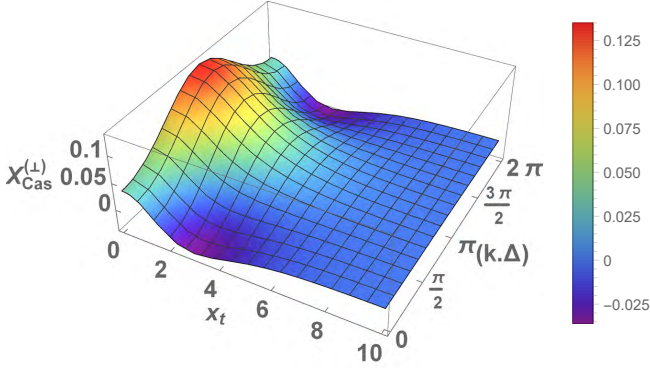


FIG. 9. (Color online) The scaling function $X_{\text{Cas}}^{(\perp)}(x_t, x_k, x_1, x_L)$ as a function of $x_t \in (0, 10]$ and $\mathbf{k} \cdot \Delta \in [0, 2\pi]$ for $x_k = 0.1$, $x_1 = 10x_L = 1$. As we see, the scaling function in that case is predominantly positive.

$X_{\text{Cas}}^{(h,\alpha)}$ can be both positive and negative, independently on the values of x_1 and/or x_L .

IV. THE 3D MEAN-FIELD XY MODEL

A. With infinite surface fields

In Ref. [55] the XY model characterized by the functional

$$\mathcal{F}[\mathbf{m}; t, L] = \int_{-L/2}^{L/2} dz \left[\frac{b}{2} \left| \frac{d\mathbf{m}}{dz} \right|^2 + \frac{1}{2} at |\mathbf{m}|^2 + \frac{1}{4} g |\mathbf{m}|^4 \right], \quad (4.1)$$

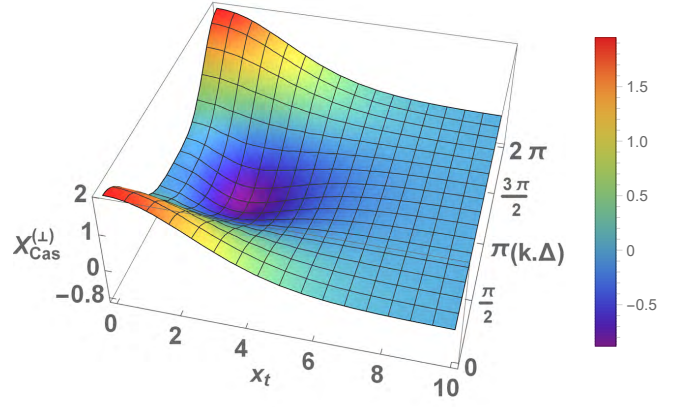


FIG. 10. (Color online) The scaling function $X_{\text{Cas}}^{(\perp)}(x_t, x_k, x_1, x_L)$ as a function of $x_t \in (0, 10]$ and $\mathbf{k} \cdot \Delta \in [0, 2\pi]$ for $x_k = 0.1$, $x_1 = -x_L = 1$. As we see, the scaling function in that case can be both positive and negative, depending on the values of its arguments.

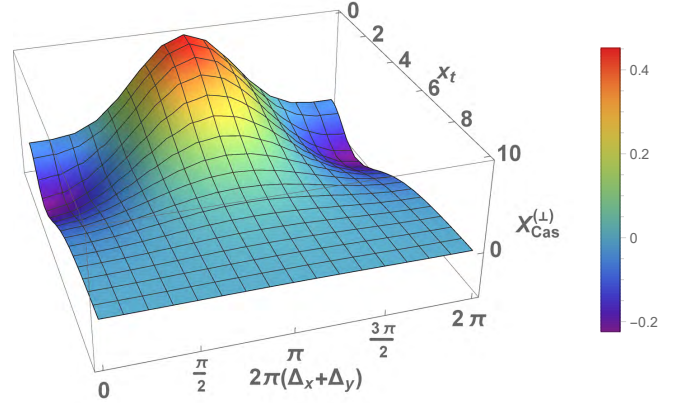


FIG. 11. (Color online) The scaling function $X_{\text{Cas}}^{(\perp)}(x_t, x_k = 0, x_1, x_L)$ as a function of $x_t \in (0, 10]$ and $\Delta_x + \Delta_y \in [0, 1]$ for $x_1 = x_L = 1$. As we see, $X_{\text{Cas}}^{(\perp)}$ can be both positive and negative, depending on the values of its arguments.

has been studied in the presence of what have been termed twisted boundary conditions.

Switching to polar coordinates,

$$\mathbf{m}(z) = (\Phi(z) \cos \varphi(z), \Phi(z) \sin \varphi(z)), \quad (4.2)$$

these boundary conditions can conveniently be defined by requiring that

$$\begin{aligned} \varphi(\pm L/2) &= \pm \alpha/2, \\ \Phi(\pm L/2) &= \infty, \end{aligned} \quad (4.3)$$

i.e., the moments at the boundaries are twisted by an angle α relative to one another. It has been shown that

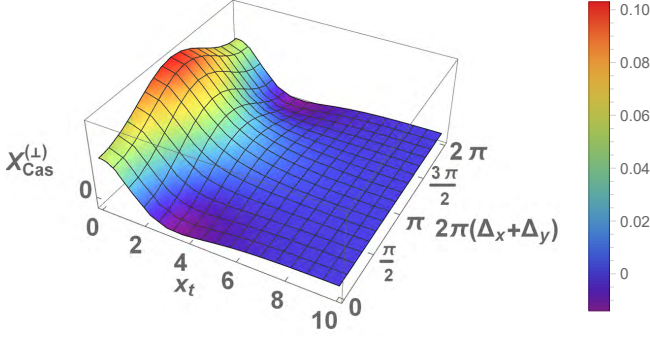


FIG. 12. (Color online) The scaling function $X_{\text{Cas}}^{(\perp)}(x_t, x_k = 0, x_1, x_L)$ as a function of $x_t \in (0, 10]$ and $\Delta_x + \Delta_y \in [0, 1]$ for $x_1 = 10x_L = 1$. As we see, the scaling function in that case is predominantly positive.

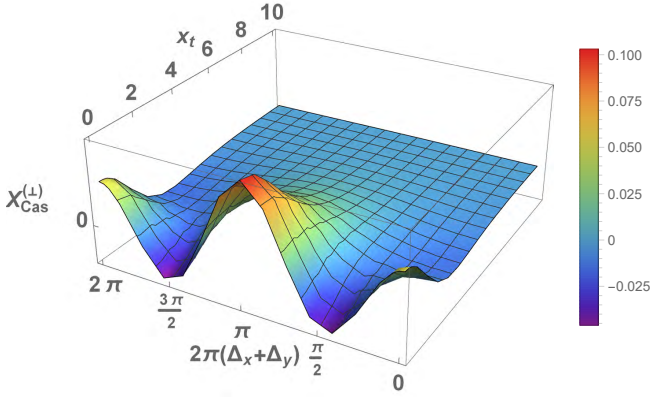


FIG. 13. (Color online) The scaling function $X_{\text{Cas}}^{(\perp)}(x_t, x_k = 0, x_1, x_L)$ as a function of $x_t \in (0, 10]$ and $\Delta_x + \Delta_y \in [0, 1]$ for $10x_1 = x_L = 1$. As we see, the scaling function in that case can be both positive and negative.

the Casimir force has the form

$$\beta F_{\text{Cas}}(t, L) = \frac{b}{\hat{g}} L^{-4} X_{\text{Cas}}^{(\alpha)}(x_t), \quad (4.4)$$

where $\hat{a} = a/b$, $\hat{g} = g/b$, $x_t = \hat{a}tL^2$ and

$$X_{\text{Cas}}^{(\alpha)}(x_t) = \begin{cases} X_0^4[p^2 - (1 + \tau)], & x_t \geq 0 \\ X_0^4[p^2 - (1 + \tau/2)^2], & x_t \leq 0 \end{cases}. \quad (4.5)$$

Here

$$\tau = x_t/X_0^2, \quad X_0 = \int_1^\infty \frac{dx}{\sqrt{(x-1)[x^2 + x(1+\tau) + p^2]}} \quad (4.6)$$

$$X_0 = \int_1^\infty \frac{dx}{\sqrt{(x-1)[x^2 + x(1+\tau) + p^2]}}, \quad (4.7)$$

and p is to be determined for any fixed value of x_t so that the twisted spins at the boundary make the prescribed angle α . Let

$$x_{\pm} = \frac{1}{2} [-(\tau + 1) \pm \sqrt{(\tau + 1)^2 - 4p^2}] \quad (4.8)$$

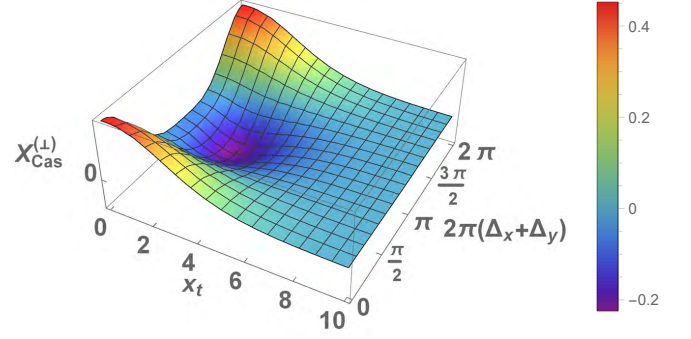


FIG. 14. (Color online) The scaling function $X_{\text{Cas}}^{(\perp)}(x_t, x_k = 0, x_1, x_L)$ as a function of $x_t \in (0, 10]$ and $\Delta_x + \Delta_y \in [0, 1]$ for $x_1 = -x_L = 1$ or $x_1 = -x_L = -1$. As we see, the scaling function in that case can be both positive and negative.

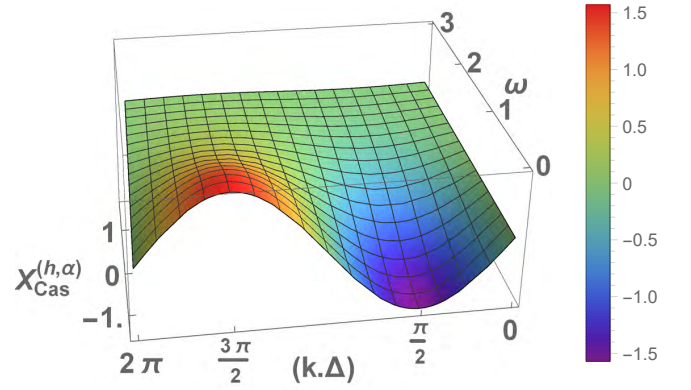


FIG. 15. (Color online) The scaling function $X_{\text{Cas}}^{(h, \alpha)}(w, x_1, x_L)$, see Eq. (3.43), as a function of $w \in (0, 3]$ and $(\mathbf{k}, \Delta) \in [0, 2\pi]$ for $x_1 = x_L = 1$.

be the roots of the quadratic term in the square brackets in the denominator of (4.7). There are two subcases: it A) the roots are real, and B) the roots are complex conjugates of each other.

A) The roots x_{\pm} are real. Then

$$X_0 = \frac{2}{\sqrt{1-x_-}} K \left[\sqrt{\frac{x_+ - x_-}{1-x_-}} \right] \quad (4.9)$$

and

$$\alpha = \frac{\sqrt{|x_- x_+|} X_0}{x_-} \left\{ 1 - \frac{2}{X_0 \sqrt{1-x_-}} \Pi \left[\frac{x_-}{x_- - 1}, \sqrt{\frac{x_+ - x_-}{1-x_-}} \right] \right\}. \quad (4.10)$$

We note that

$$\tau = -1 - x_- - x_+, \quad p = \sqrt{|x_- x_+|}. \quad (4.11)$$

B) The roots x_{\pm} are complex.

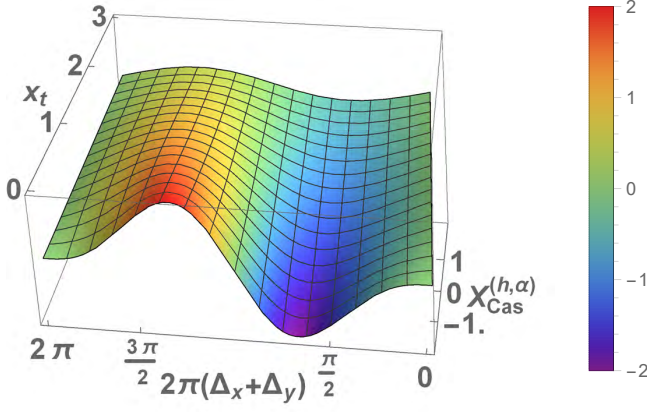


FIG. 16. (Color online) The scaling function $X_{\text{Cas}}^{(h, \alpha)}(x_t, x_1, x_L)$, see Eq. (3.44), as a function of $w \in (0, 3]$ and $\Delta_x + \Delta_y \in [0, 1]$ for $x_1 = x_L = 1$. Let us remind that in this sub-case $\omega = x_t/2$.

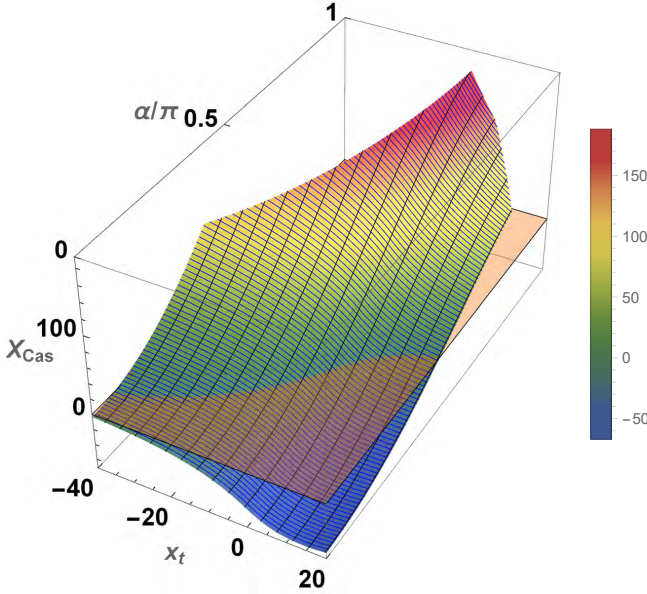


FIG. 17. (Color online) The scaling function $X_{\text{Cas}}^{(\alpha)}(x_t)$ of the XY model under twisted boundary conditions as a function of x_t and α for $h = 0$. The plane surface marks the $X_{\text{Cas}}^{(\alpha)}(x_t) = 0$ value of the force: the force is repulsive above it and attractive below it.

One has

$$X_0 = \frac{2}{\sqrt{r}} K(w), \quad (4.12)$$

and

$$\alpha = \frac{pX_0}{1-r} + \frac{4p}{r^2-1} \sqrt{\frac{r}{1-w^2}} \times \Pi \left[\left(\frac{r-1}{r+1} \right)^2, \frac{w}{\sqrt{w^2-1}} \right]. \quad (4.13)$$

where

$$r \equiv r(x_-, x_+) = \sqrt{(1-x_-)(1-x_+)} = \sqrt{2+\tau+p^2}, \quad (4.14)$$

and

$$w^2 \equiv w^2(x_-, x_+) = \frac{1}{2} + \frac{\frac{x_-+x_+}{2} - 1}{2\sqrt{(1-x_-)(1-x_+)}} = \frac{1}{2} \left(1 - \frac{3+\tau}{2\sqrt{2+\tau+p^2}} \right). \quad (4.15)$$

The scaling function $X_{\text{Cas}}^{(\alpha)}(x_t)$ of the XY model under twisted boundary conditions as a function of x_t and α is shown in Fig. 17. We recall that, as shown in Ref. [55] the asymptotic expression for $X_{\text{Cas}}^{(\alpha)}(x_t)$

$$X_{\text{Cas}}^{(\alpha)}(x_t) \simeq \frac{1}{2} \alpha^2 \left[|x_t| + 4\sqrt{2}|x_t| + \frac{1}{2} (48 - 3\alpha^2) \right], \quad (4.16)$$

when $x_t \rightarrow -\infty$. According to Eq. (4.4) the last implies that in this regime

$$\beta F_{\text{Cas}}(t, L) \simeq \frac{1}{2} \alpha^2 \frac{b}{g} |x_t| L^{-4} = \frac{1}{2} \frac{ab}{g} \alpha^2 |t| L^{-2}, \quad (4.17)$$

i.e., its leading behavior is of the order of L^{-2} there due to the existence of helicity within the system.

B. With finite surface fields

The model described immediately above constrains the spins at the surface of the film to point in particular directions. The physical realization of a such a system is much more likely to be one in which the spins at the surfaces to be under the influence of finite surface fields. Here, we consider a model for such a system. In order to do so, we employ the approach utilized in Section II of [55], in which the spin system occupies sites on a lattice that is infinite in extent in two directions and that consists a finite number of layers (here labeled 1 to L) in the third dimension. We impose surface fields that couple in the standard way to the spins on the leftmost layer, labeled 1, and the rightmost layer, labeled L . The magnitude of each of those fields is h_s , and the angle between them is α . In our mean field approach, the free energy is minimized by adjusting the expectation value of the amplitude and direction of the spins in each layer. The Casimir force follows from the difference between the free energies with L and $L+1$ layers; because of the numerical nature of the free energy results, we are unable to take the derivative with respect to film thickness, as in Section II.

We find that the Casimir force is consistent with the following scaling form

$$F_{\text{Cas}} = L^{-4} f(tL^2, h_c L) \quad (4.18)$$

where t is the bulk reduced temperature. Furthermore, for small enough h_c and t higher than the value at which the film orders spontaneously, the function f on the right hand side of (4.18) has the form

$$f(tL^2, h_cL) = f_0(tL^2) + f_1(tL^2)(h_cL)^2 + O((h_cL)^4) \quad (4.19)$$

Because of this, it is possible to envision for small h_s the behavior of the Casimir force that one encounters in the Gaussian model.

Figure 18 is a plot of the scaled Casimir force versus the scaled reduced temperature and scaled surface fields for two values of the film thickness, L . The perspective highlights the departure from the behavior in (4.19) that occurs when the temperature is sufficiently far below the bulk critical temperature that the moments in the film order spontaneously. The films in question consists of $L = 50$ and $L = 100$ layers, and the angle between the two surface fields is $\alpha = \pi/3$. As is clear from the figure, the difference between the two plots is quite small.

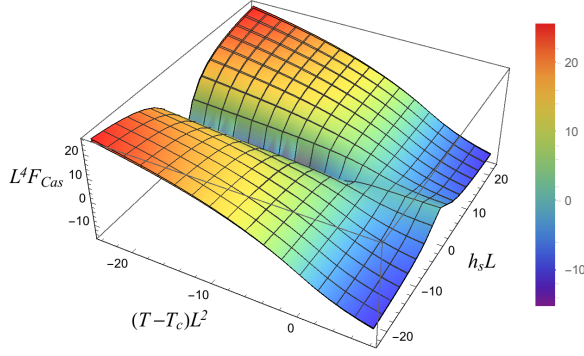


FIG. 18. (Color online) Scaled Casimir force, $L^4 F_{\text{Cas}}$, as a function of the scaled reduced temperature, tL^2 and scaled surface field amplitude, $h_s L$. The number of layers in the two films are $L = 50$ and $L = 100$, and α , the angle between the surface fields, is $\pi/3$. The difference between the two plots is barely discernible, indicating that the difference between the scaling function for $L = 50$ and the infinite L limit is quite small.

As indicated in Fig. 18, $L = 50$ is sufficiently large that the difference between the function and the scaling limit is quite small. Figure 19 illustrates the dependence of the scaled Casimir force on the scaled surface field amplitude for various values of the scaled reduced temperature. For all reduced temperatures greater than $-\pi^2$, the initial dependence on scaled surface fields is quadratic, consistent with (4.19). In fact for temperatures at and above the bulk critical temperature ($t \geq 0$) the second term in the right hand side of (4.19) is the leading non-zero contribution to that expansion. This is consistent with the amplification of the Casimir force that one finds in the Gaussian model—see Section III. However, such amplification only occurs when there is spontaneous ordering in the film. Figure 20 shows the scaled Casimir force

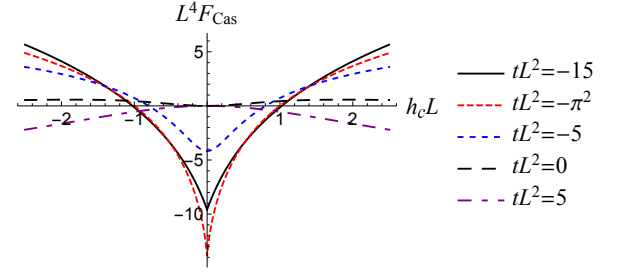


FIG. 19. (Color online) Scaled Casimir force, $L^4 F_{\text{Cas}}$, as a function of the scaled surface field, $h_s L$ for various scaled reduced temperatures, tL^2 . Here, $L = 50$ and $\alpha = \pi/3$. When $tL^2 > -\pi^2$ the small h_s dependence of the Casimir force is quadratic, consistent with (4.19). Below that value of the scaled reduced temperature, the small h_s dependence is linear in the absolute value of that quantity, as exemplified by the curve for $tL^2 = -15$.

as a function of the scaled surface field for $tL^2 = 5$ and $tL^2 = -5$, above and below the bulk transition but above the threshold for film ordering. This plot illustrates the saturation of the Casimir force when the reduced temperature is above the threshold for film ordering, $tL^2 = -\pi^2$. The Casimir force changes sign as L increases for fixed

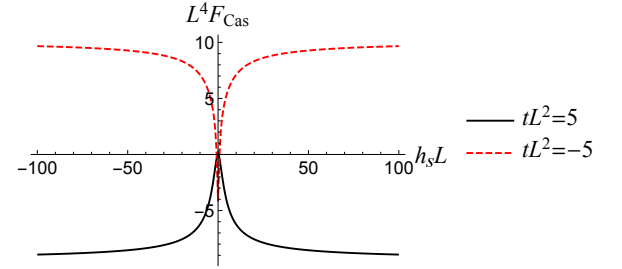


FIG. 20. (Color online) Dependence of the scaled Casimir force on the scaled surface field for two values of scaled reduced temperature above the point, $tL^2 = -\pi^2$, at which spontaneous ordering occurs in the film. Here, $L = 50$ and $\alpha = \pi/3$. The plots illustrate the saturation of the influence of the surface fields, at odds with the amplification effect seen in Section III. The figure also illustrates the fact that the Casimir force can change sign as the temperature is varied. This is due to the fact that there is a range of temperatures below the bulk critical temperature in which the bulk system orders while the film remains disordered. For $T > T_c$ both the bulk and the finite system are disordered. For $|h_s| \gg 1$ the Casimir force approaches its value for fixed boundary conditions, the case considered in Subsection IV A.

α , T and h_s . This is displayed in Fig. 21. We also note that the force changes sign for moderate values of L . It can readily be established that the overall behavior of the Casimir force is in accord with Eq. (4.19); see, for instance, Fig. 20.

If spontaneous ordering is possible, then amplification of the Casimir force does occur. Figure 22 plots the newly

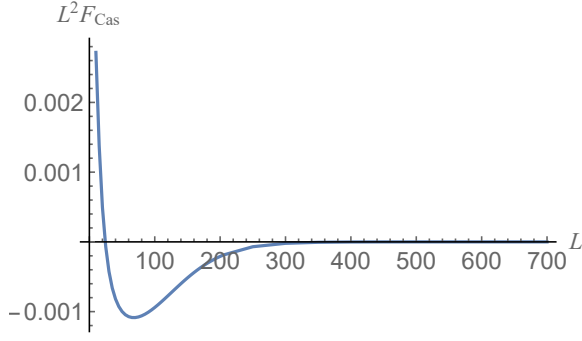


FIG. 21. (Color online) Scaled Casimir force, $L^2 F_{\text{Cas}}$, as a function of L , for fixed values of temperature $t = 0.001$, helicity $\alpha = \pi/3$ and value of the surface field amplitude $h_s = 0.1$.

scaled Casimir force $L^2 F_{\text{Cas}}$ against system size L , illustrating the enhanced force amplitude as a function of system size, L , expressed in terms of the scaled variable tL^2 . Here, the reduced temperature is fixed at $t = -0.05$, while the surface field amplitudes are set to 0.05, $\alpha = \pi/3$ and the system size varies from $L = 2$ to $L = 3,000$. The behavior displayed is a direct result of the energy stored in the helical spin configuration, a response to the surface fields that are tilted with respect to each other. Of addi-

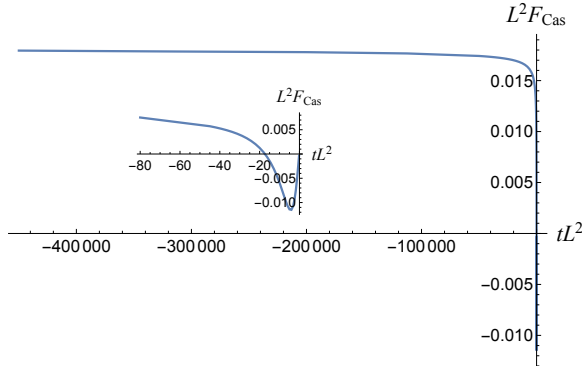


FIG. 22. (Color online) Illustrating the L dependence of the Casimir force for a negative value of reduced temperature, $t = -0.05$ with surface field amplitude $h_s = 0.05$ and $\alpha = \pi/3$. The plot is generated by varying the film thickness L for fixed values of t , h_s and α . The large graph shows how $L^2 F_{\text{Cas}}$ varies over an extended range of film thicknesses L , and the inset shows the L dependence over a much smaller range.

tional interest in this plot is the variation of the Casimir

force for smaller values of L , shown in the inset. Note the change in the sign of the Casimir force. A Casimir force going as L^{-2} is consistent with the energy associated with a helicity modulus, which is natural given that the XY system supports such a modulus in the regime in which it spontaneously orders. In this case the surface fields play the essential role of enforcing a helical structure on the order parameter when spontaneous ordering occurs.

The enhanced Casimir force is consistent with the scaling form of (4.18). Figure 23 displays the dependence of the scaled Casimir force $L^4 F_{\text{Cas}}$ on the scaled variable tL^2 . An important feature of this plot is its linear de-

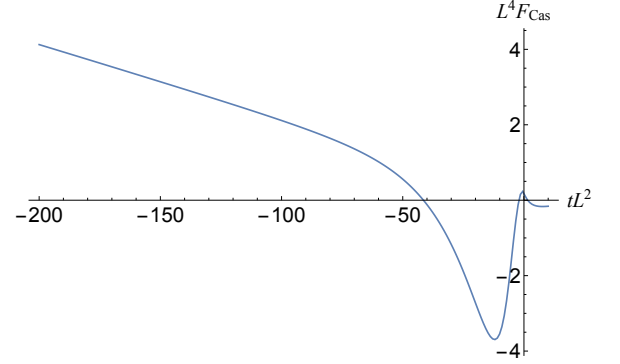


FIG. 23. (Color online) The scaled Casimir force, $L^4 F_{\text{Cas}}$, as a function of the scaled variable tL^2 . The thickness of the film is $L = 50$, the surface field amplitudes have been set to 0.01 and the angle between them, α , is $\pi/3$.

pendence on the scaled reduced temperature when it is sizable and negative. This leads to an overall L dependence going as L^{-2} . Another significant property of the critical Casimir force plotted in Fig. 23 is its change in sign in the vicinity of the bulk critical point. In this sense, the Casimir force is tunable—and can be changed from attractive to repulsive—through a variation in temperature.

Finally, Fig. 24 displays the dependence of the scaled Casimir force, $L^4 F_{\text{Cas}}$, on scaled reduced temperature, tL^2 and scaled surface field amplitude, $h_s L$ for a variety of values of the angular difference, α , between the two surface fields. As shown in the plots, when α increases from 0 to π the minimum of the force becomes shallower and the region of parameters tL^2 and $h_s L$ in which the force is repulsive expands. We also note that the amplitude of the force for any fixed combination of the parameters tL^2 and $h_s L$ is a monotonically increasing function of α . The force is attractive in the whole region of $h_s L$ and tL^2 values only for $\alpha = 0$.

V. DISCUSSION AND CONCLUDING REMARKS

The Casimir force has provided an unexpectedly rich and varied set of phenomena for study and potential ex-

ploitation. In this paper, we have attempted to demonstrate that interactions between the bounding system and

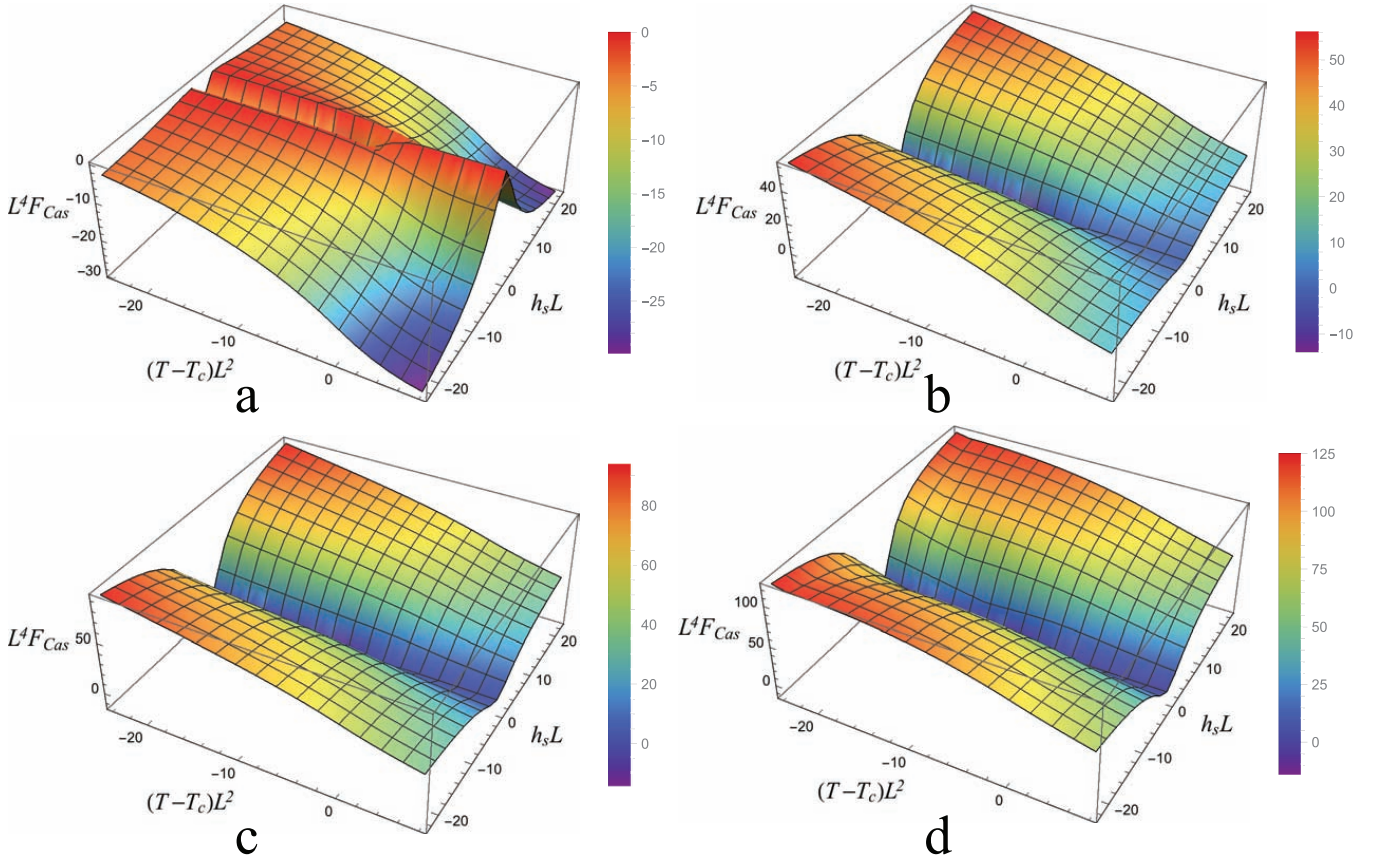


FIG. 24. (Color online) Scaled Casimir force, $L^4 F_{\text{Cas}}$, as a function of the scaled reduced temperature, tL^2 and scaled surface field amplitude, $h_s L$. The number of layers in the film is $L = 50$. The values of α , the angle between the surface fields are, reading left to right and then top to bottom are **a**: 0, **b**: $\pi/2$, **c**: $2\pi/3$ and **d**: π .

the media that supports the Casimir force allow for the possibility of utilizing those interactions, here parameterized as surface fields, to control—and in certain cases greatly amplify—that force. Our focus has been the critical Casimir force, but a number of our results extend far beyond the critical regime. We find that the angle between surface fields can significantly affect the magnitude and the sign of the Casimir force, that variations in temperature can also have such an effect, and that the strength of the critical Casimir force can undergo substantial amplification as a consequence of the application of surface fields. Such fields represent a useful and likely accurate quantification of the action of modifications of the structure or composition of bounding surfaces in the medium giving rise to the Casimir force. Thus, the results presented here could well be utilized or expanded upon to motivate experimental investigations of the effects of surface patterning on the Casimir force.

The key findings reported here are twofold. First, the combination of helicity and surface fields allows for the manipulation of both the sign and the amplitude of the Casimir force. In certain circumstances—particularly when the system supports helicity in the bulk—the force

can be greatly amplified in magnitude. The second finding is that the expressions describing the Casimir force are consistent with the expectations of finite size scaling, as embodied in Eqs. (2.11), (2.20), (3.20), (3.32), (3.42), (4.4) and (4.18).

One possible setting for an experimental study might be a nematic liquid crystal film. Here, the order parameter is quadrupolar, rather than dipolar as in the case of the XY or Heisenberg models, but the continuous symmetry with respect to rotation of the order parameter is nevertheless in the same general class as in the systems considered here. In fact, a class of Liquid Crystal Display (LCD) devices operates on the basis of inducing of a helical structure in liquid crystalline films [63]. It is also possible that the results reported here are applicable to the case of a liquid Helium film in the superfluid state in which a temperature gradient exists between the substrate on which the film has condensed and that gas phase bordering its free surface. Such a temperature gradient induces flow in the superfluid component, which entails a rotation of the superfluid wave function in the complex plane [64, 65].

The models investigated here are unlikely to be directly

realized in nature, either because of their low dimensionality, or because they neglect important phenomena such as saturation of the order parameter as in the Gaussian model or are based on approximations, such as the mean field theory. Nevertheless, we are confident in the overall import of our results: that surface fields and helicity in the medium that generates the Casimir force are likely to prove quite significant as experimentally accessible modifiers of that force. How those surface fields are to be generated will vary from system to system, but there is every reason to anticipate that ways will be found and that the result will be a greater insight into the Casimir force and, one hopes, new and useful applications of this interaction.

ACKNOWLEDGMENTS

D.D. gratefully acknowledges the financial support via contract DN02/8 of Bulgarian NSF. J. R. is pleased to acknowledge support from the NSF through DMR Grant No. 1006128

Appendix A: Calculation of the free energy for the 1d XY model with boundary fields

The simplest way we are aware of for calculation of the free energy of the 1d XY model is based on the identities

[66, 67]

$$e^{z \cos \theta} = \sum_{n=-\infty}^{\infty} e^{in\theta} I_n(z) \quad (\text{A1})$$

and

$$\delta_{n,0} = \frac{1}{2\pi} \int_0^{2\pi} e^{in\theta} d\theta. \quad (\text{A2})$$

From Eqs. (2.4) and (B3) one then obtains

$$\exp(-\beta F_N) = \int_0^{2\pi} \prod_{i=1}^N \frac{d\varphi_i}{2\pi} \times \quad (\text{A3})$$

$$\sum_{n_1=-\infty}^{\infty} e^{in_1(\psi_1-\varphi_1)} I_{n_1}(h_1) \sum_{n_2=-\infty}^{\infty} e^{in_2(\varphi_1-\varphi_2)} I_{n_2}(K) \times \dots \times \sum_{n_{N-1}=-\infty}^{\infty} e^{in_{N-1}(\varphi_{N-1}-\varphi_N)} I_{n_{N-1}}(K) \times \quad (\text{A4})$$

$$\sum_{n_N=-\infty}^{\infty} e^{in_N(\varphi_N-\psi_N)} I_{n_N}(h_N), \quad (\text{A5})$$

wherefrom, using Eq. (A2), one obtains Eq. (2.6). Obviously, Eq. (2.6) can be written in the form

$$\exp(-\beta F_N) = I_0(h_1) I_0(K)^{N-1} I_0(h_N) \times \left[1 + 2 \sum_{k=1}^{\infty} \cos(k\psi) \frac{I_k(h_1)}{I_0(h_1)} \left(\frac{I_k(K)}{I_0(K)} \right)^{N-1} \frac{I_k(h_N)}{I_0(h_N)} \right]. \quad (\text{A6})$$

From Eq. (A6) for the total pressure

$$\beta F_{\text{tot}} = -\frac{\partial}{\partial N} [\beta F_N] \quad (\text{A7})$$

exerted by the end points on the system one then obtains

$$\beta F_{\text{tot}} = \ln I_0(K) + \frac{2 \sum_{k=1}^{\infty} \cos[k(\psi_1 - \psi_2)] \log \left[\frac{I_k(K)}{I_0(K)} \right] \frac{I_k(h_1)}{I_0(h_1)} \left(\frac{I_k(K)}{I_0(K)} \right)^{N-1} \frac{I_k(h_N)}{I_0(h_N)}}{1 + 2 \sum_{k=1}^{\infty} \cos[k(\psi_1 - \psi_2)] \frac{I_k(h_1)}{I_0(h_1)} \left(\frac{I_k(K)}{I_0(K)} \right)^{N-1} \frac{I_k(h_N)}{I_0(h_N)}}, \quad (\text{A8})$$

wherefrom one immediately derives the expression (2.8) for the Casimir force given in the main text.

Using the Poisson identity

$$\sum_{k=-\infty}^{\infty} \exp(ika - k^2b) = \sqrt{\frac{\pi}{b}} \sum_{n=-\infty}^{\infty} \exp \left[-\frac{(2\pi n + a)^2}{4b} \right] \quad (\text{A9})$$

one can derive expressions for the scaling function of the Casimir force convenient for values of the scaling variable x ranging from moderate to large values of x and one convenient for small values of x .

Appendix B: Calculation of the free energy for the 1d Heisenberg model with boundary fields

Let us write the vectors in Eq. (2.3) in spherical coordinates supposing the spin chain to be along the x axis. One has

$$\mathbf{H}_1 = H_1 \{ \sin \varphi_1^h \cos \theta_1^h, \sin \varphi_1^h \sin \theta_1^h, \cos \varphi_1^h \} \quad (\text{B1})$$

$$\mathbf{H}_N = H_N \{ \sin \varphi_N^h \cos \theta_N^h, \sin \varphi_N^h \sin \theta_N^h, \cos \varphi_N^h \}$$

$$\mathbf{S}_i = \{ \sin \varphi_i \cos \theta_i, \sin \varphi_i \sin \theta_i, \cos \varphi_i \}, i = 1, \dots, N.$$

Then for the scalar products one obtains

$$\begin{aligned}
\mathbf{H}_1 \cdot \mathbf{S}_1 &= H_1 [\sin \varphi_1^h \sin \varphi_1 \cos (\theta_1^h - \theta_1) + \\
&\quad \cos \varphi_1^h \cos \varphi_1] \equiv H_1 \cos \psi_1, \\
\mathbf{H}_N \cdot \mathbf{S}_N &= H_N [\sin \varphi_N^h \sin \varphi_N \cos (\theta_N^h - \theta_N) + \\
&\quad \cos \varphi_N^h \cos \varphi_N] \equiv H_N \cos \psi_N, \\
\mathbf{S}_i \cdot \mathbf{S}_{i+1} &= \sin \varphi_i \sin \varphi_{i+1} \cos (\theta_i - \theta_{i+1}) + \\
&\quad \cos \varphi_i \cos \varphi_{i+1} \equiv \cos \phi_i,
\end{aligned} \tag{B2}$$

where the angle ϕ_i , $i = 1, \dots, N-1$ is between the spins \mathbf{S}_i and \mathbf{S}_{i+1} , and the angles ψ_1 and ψ_N are between the vectors \mathbf{H}_1 and \mathbf{S}_1 , and the vectors \mathbf{H}_N and \mathbf{S}_N , respectively.

The free energy $-\beta F_N$ of this system is

$$\exp(-\beta F_N) = \int_0^{2\pi} \prod_{i=1}^N \frac{d\theta_i}{4\pi} \int_0^\pi \prod_{i=1}^N d\varphi_i \sin \varphi_i \exp(-\beta \mathcal{H}), \tag{B3}$$

where the normalization is over the solid angle 4π because

$$\int_0^{2\pi} d\theta \int_0^\pi d\varphi \sin \varphi = 4\pi. \tag{B4}$$

In order to perform the integrations we use the expansion

$$e^{z \cos \theta} = \sqrt{\frac{\pi}{2z}} \sum_{n=0}^{\infty} (2n+1) I_{n+1/2}(z) P_n(\cos \theta) \tag{B5}$$

combined with the addition theorem for the spherical harmonics [66, 67]

$$P_n(\cos \phi_i) = \frac{4\pi}{2n+1} \times \sum_{m=-n}^n Y_{n,m}^*(\varphi_{i+1}, \theta_{i+1}) Y_{n,m}(\varphi_i, \theta_i). \tag{B6}$$

Here $I_{n+1/2}(z)$ is the modified Bessel function of the first kind, $P_n(x)$ is the Legendre polynomial of degree n and $Y_{n,m}(\phi, \theta)$ is the spherical harmonic. We remind the orthogonality relation that holds for the spherical harmonics

$$\int_0^\pi d\varphi \int_0^{2\pi} d\theta \sin \varphi Y_{l_1, m_1}(\varphi, \theta) Y_{l_2, m_2}^*(\varphi, \theta) = \delta_{l_1, l_2} \delta_{m_1, m_2}. \tag{B7}$$

From Eq. (B3) we obtain

$$\begin{aligned} \exp(-\beta F_N) &= \int_0^{2\pi} \prod_{i=1}^N \frac{d\theta_i}{4\pi} \int_0^\pi \prod_{i=1}^N d\varphi_i \sin \varphi_i \\ &\quad \times e^{h_1 \cos \psi_1} \left(\prod_{i=1}^{N-1} e^{K \cos \phi_i} \right) e^{h_N \cos \psi_N}, \end{aligned} \tag{B8}$$

where K , h_1 and h_N are defined in accord with Eq. (2.17). Now we have to take into account that, according to Eqs. (B5) and (B6),

$$\begin{aligned} e^{h_1 \cos \psi_1} &= \sqrt{\frac{\pi}{2h_1}} \sum_{n_1=0}^{\infty} (2n_1+1) I_{n_1+1/2}(h_1) P_{n_1}(\cos \psi_1) \\ &= (4\pi) \sqrt{\frac{\pi}{2h_1}} \times \sum_{n_1=0}^{\infty} I_{n_1+1/2}(h_1) \sum_{m_1=-n_1}^{n_1} Y_{n_1, m_1}^*(\varphi_1, \theta_1) Y_{n_1, m_1}(\varphi_1^h, \theta_1^h), \end{aligned} \tag{B9}$$

$$\begin{aligned} e^{h_N \cos \psi_N} &= \sqrt{\frac{\pi}{2h_N}} \sum_{n_N=0}^{\infty} (2n_N+1) I_{n_N+1/2}(h_N) P_{n_N}(\cos \psi_N) \\ &= (4\pi) \sqrt{\frac{\pi}{2h_N}} \times \sum_{n_N=0}^{\infty} I_{n_N+1/2}(h_N) \sum_{m_N=-n_N}^{n_N} Y_{n_N, m_N}^*(\varphi_N^h, \theta_N^h) Y_{n_N, m_N}(\varphi_N, \theta_N), \end{aligned} \tag{B10}$$

and

$$e^{K \cos \phi_i} = \sqrt{\frac{\pi}{2K}} \sum_{n_{i+1}=0}^{\infty} (2n_{i+1}+1) I_{n_{i+1}+1/2}(K) P_{n_{i+1}}(\cos \phi_i) \tag{B11}$$

$$= (4\pi) \sqrt{\frac{\pi}{2K}} \sum_{n_{i+1}=0}^{\infty} I_{n_{i+1}+1/2}(K) \sum_{m_{i+1}=-n_{i+1}}^{n_{i+1}} Y_{n_{i+1}, m_{i+1}}^*(\varphi_{i+1}, \theta_{i+1}) Y_{n_{i+1}, m_{i+1}}(\varphi_i, \theta_i), \tag{B12}$$

with $i = 1, \dots, N-1$. Inserting the above expression into Eq. (B8) one can easily perform the integration over φ_i and θ_i , $i = 1, \dots, N$ taking into account

the orthogonality relations Eq. (B7). One derives that $n_1 = n_2 = \dots = n_N = n$, and $m_1 = m_2 = \dots = m_N = m$ and, thus, from Eq. (B8) we obtain

$$\begin{aligned}
\exp(-\beta F_N) &= (4\pi) \sqrt{\frac{\pi}{2h_1}} \sqrt{\frac{\pi}{2h_N}} \left(\sqrt{\frac{\pi}{2K}} \right)^{N-1} \\
&\sum_{n=0}^{\infty} I_{n+1/2}(h_1) I_{n+1/2}(h_N) [I_{n+1/2}(K)]^{N-1} \sum_{m=-n}^n Y_{n,m}(\varphi_1^h, \theta_1^h) Y_{n,m}^*(\varphi_N^h, \theta_N^h) \\
&= \left(\frac{\pi}{2K} \right)^{(N-1)/2} \frac{\pi}{2\sqrt{h_1 h_N}} \sum_{n=0}^{\infty} (2n+1) P_n(\cos \psi_h) I_{n+1/2}(h_1) I_{n+1/2}(h_N) [I_{n+1/2}(K)]^{N-1},
\end{aligned} \tag{B13}$$

where, in the last line, we have again used the addition theorem for the spherical harmonics Eq. (B6). In Eq. (B13) ψ_h is the angle between the vectors \mathbf{H}_1 and \mathbf{H}_N where

$$\cos \psi_h = \sin \varphi_1^h \sin \varphi_N^h \cos(\theta_1^h - \theta_N^h) + \cos \varphi_1^h \cos \varphi_N^h. \tag{B14}$$

From Eq. (B13) and Eq. (2.16) for the total pressure exerted by the end points on the system one derives

$$\beta F_{\text{tot}} \equiv -\frac{\partial}{\partial N} [\beta F_N] = \ln \left[\frac{\sinh K}{K} \right] + \frac{\sum_{n=1}^{\infty} (2n+1) P_n(\cos \psi_h) \ln \left[\frac{I_{n+1/2}(K)}{I_{1/2}(K)} \right] \frac{I_{n+1/2}(h_1)}{I_{1/2}(h_1)} \frac{I_{n+1/2}(h_N)}{I_{1/2}(h_N)} \left[\frac{I_{n+1/2}(K)}{I_{1/2}(K)} \right]^{N-1}}{1 + \sum_{n=1}^{\infty} (2n+1) P_n(\cos \psi_h) \frac{I_{n+1/2}(h_1)}{I_{1/2}(h_1)} \frac{I_{n+1/2}(h_N)}{I_{1/2}(h_N)} \left[\frac{I_{n+1/2}(K)}{I_{1/2}(K)} \right]^{N-1}}. \tag{B15}$$

From here one derives the exact result for the Casimir force reported in Eq. (2.19) in the main text. From it one can extract the corresponding scaling behavior reported in Eq. (2.22) which is convenient for evaluation of the behavior of the force for moderate and large values of

the scaling variable x . Here we present the corresponding derivation of the representation convenient for extracting the behavior of the force for small values of the scaling variable. Let us start by considering the sum

$$\begin{aligned}
S(\psi_h, h_1, h_N, K) &\equiv \sum_{n=1}^{\infty} (2n+1) P_n(\cos \psi_h) \frac{I_{n+1/2}(h_1)}{I_{1/2}(h_1)} \frac{I_{n+1/2}(h_N)}{I_{1/2}(h_N)} \left[\frac{I_{n+1/2}(K)}{I_{1/2}(K)} \right]^{N-1} \\
&\simeq \sum_{n=1}^{\infty} (2n+1) P_n(\cos \psi_h) \frac{e^{h_1 - (n+1/2)^2/(2h_1)}}{\sqrt{2\pi h_1} I_{1/2}(h_1)} \frac{e^{h_N - (n+1/2)^2/(2h_N)}}{\sqrt{2\pi h_N} I_{1/2}(h_N)} \left[\frac{e^{K - (n+1/2)^2/(2K)}}{\sqrt{2\pi K} I_{1/2}(K)} \right]^{N-1} \\
&\simeq \sum_{n=1}^{\infty} (2n+1) P_n(\cos \psi_h) \frac{\exp \left[-\frac{1}{2} (n+1/2)^2 \left(\frac{1}{h_1} + \frac{1}{h_N} + \frac{N-1}{K} \right) \right]}{\exp \left[-\frac{1}{2} (1/2)^2 \left(\frac{1}{h_1} + \frac{1}{h_N} + \frac{N-1}{K} \right) \right]} \\
&\simeq \sum_{n=1}^{\infty} (2n+1) P_n(\cos \psi_h) \frac{I_{n+1/2} \left(\frac{1}{h_{\text{eff}} + x} \right)}{I_{1/2} \left(\frac{1}{h_{\text{eff}} + x} \right)} = \sum_{n=0}^{\infty} (2n+1) P_n(\cos \psi_h) \frac{I_{n+1/2} \left(\frac{1}{h_{\text{eff}} + x} \right)}{I_{1/2} \left(\frac{1}{h_{\text{eff}} + x} \right)} - 1 \\
&= \sqrt{\frac{2}{\pi (h_{\text{eff}}^{-1} + x)}} \frac{\exp \left[\frac{\cos \psi_h}{h_{\text{eff}}^{-1} + x} \right]}{I_{1/2} \left(\frac{1}{h_{\text{eff}} + x} \right)} - 1 = \frac{1}{(h_{\text{eff}}^{-1} + x)} \frac{\exp \left[\frac{\cos \psi_h}{h_{\text{eff}}^{-1} + x} \right]}{\sinh \left(\frac{1}{h_{\text{eff}} + x} \right)} - 1.
\end{aligned} \tag{B16}$$

Appendix C: Calculation of the free energy for the 3d Gaussian model

In the current appendix we will outline some technical steps needed to obtain the free energy of the Gaussian

model under the considered boundary conditions.

Performing the Fourier transform

$$S_{x,y,z} = \frac{1}{\sqrt{M}} \sum_{m=1}^M \left[\cos\left(\frac{2\pi}{M}mx\right) + \sin\left(\frac{2\pi}{M}mx\right) \right] \\ \times \frac{1}{\sqrt{N}} \sum_{n=1}^N \left[\cos\left(\frac{2\pi}{N}ny\right) + \sin\left(\frac{2\pi}{N}ny\right) \right] \\ \times \sqrt{\frac{2}{L+1}} \sum_{l=1}^L \sin\left(\frac{\pi}{L+1}lz\right) \tilde{S}_{m,n,l} \quad (C1)$$

in Eq. (3.4), one can easily diagonalize the Hamiltonian. Then, performing the integrations over $\tilde{S}_{m,n,l}$, $m = 1, \dots, M$, $n = 1, \dots, N$ and $l = 1, \dots, L$ one immediately obtains Eqs. (3.11) and (3.12) for the field-independent and field-dependent parts of the free energy reported in the main text. In what follows we explain how to perform the summations in these terms. We start with the term that depends on the applied surface fields.

1. Evaluation of the field dependent term

Taking L , for definiteness, to be odd number, we start by rewriting Eq. (3.11) in the form

$$\Delta F_h = \Delta F_h^{\text{odd}} + \Delta F_h^{\text{even}}, \quad (C2)$$

where

i) if $p \neq M$ or $q \neq N$:

$$-\beta \Delta F_h^{\text{even}} = \frac{MN}{8(L+1)K^\perp} S^{\text{even}}(\Lambda, L) \times \quad (C3) \\ [h_1^2 + h_L^2 - 2h_L h_1 \cos(\mathbf{k} \cdot \mathbf{\Delta})],$$

and

$$-\beta \Delta F_h^{\text{odd}} = \frac{MN}{8(L+1)K^\perp} S^{\text{odd}}(\Lambda, L) \times \quad (C4) \\ [h_1^2 + h_L^2 + 2h_L h_1 \cos(\mathbf{k} \cdot \mathbf{\Delta})],$$

ii) if $p = M$ and $q = N$

$$-\beta \Delta F_h^{\text{even}} = \frac{MN}{8(L+1)K^\perp} S^{\text{even}}(\Lambda, L) \times \quad (C5) \\ [h_1 - h_L \cos 2\pi(\Delta_x + \Delta_y)]^2,$$

and

$$-\beta \Delta F_h^{\text{odd}} = \frac{MN}{8(L+1)K^\perp} S^{\text{odd}}(\Lambda, L) \times \quad (C6) \\ [h_1 + h_L \cos 2\pi(\Delta_x + \Delta_y)]^2.$$

In the above expressions

$$S^{\text{even}}(\Lambda, L) = \sum_{l=1}^{(L-1)/2} \frac{\sin^2\left(\frac{2\pi l}{L+1}\right)}{\Lambda - \cos\left(\frac{2\pi l}{L+1}\right)}, \quad (C7)$$

$$S^{\text{odd}}(\Lambda, L) = \sum_{l=1}^{(L-1)/2} \frac{\sin^2\left(\frac{\pi(2l+1)}{L+1}\right)}{\Lambda - \cos\left(\frac{\pi(2l+1)}{L+1}\right)}, \quad (C8)$$

and

$$\Lambda = 1 + \left(\frac{\beta_c}{\beta} - 1\right) \left[2\frac{J^\parallel}{J^\perp} + 1\right] \\ + \frac{J^\parallel}{J^\perp} \left[2 - \cos\left(\frac{2\pi p}{M}\right) - \cos\left(\frac{2\pi q}{N}\right)\right]. \quad (C9)$$

It is easy to show that

$$S^{\text{even}}(\Lambda, L) = \frac{1}{2}(L-1)\Lambda + (1-\Lambda^2)\hat{S}^{\text{even}}(\Lambda, L) \quad (C10)$$

where

$$\hat{S}^{\text{even}}(\Lambda, L) = \sum_{l=1}^{(L-1)/2} \frac{1}{\Lambda - \cos\left(\frac{2\pi l}{L+1}\right)} \quad (C11)$$

and that

$$S^{\text{odd}}(\Lambda, L) = \frac{1}{2}(L+1)\Lambda + (1-\Lambda^2)\hat{S}^{\text{odd}}(\Lambda, L) \quad (C12)$$

where

$$\hat{S}^{\text{odd}}(\Lambda, L) = \sum_{l=1}^{(L-1)/2} \frac{1}{\Lambda - \cos\left(\frac{\pi(2l+1)}{L+1}\right)}. \quad (C13)$$

The summations in Eq. (C11) and Eq. (C13) can be performed using [68] the identities

$$\cosh nx - \cos ny = 2^{n-1} \prod_{k=0}^{n-1} \left[\cosh x - \cos\left(y + \frac{2\pi k}{n}\right) \right] \quad (C14)$$

and

$$\cos nx - \cos ny = 2^{n-1} \prod_{k=0}^{n-1} \left[\cos x - \cos\left(y + \frac{2\pi k}{n}\right) \right]. \quad (C15)$$

With the help of the variable λ , introduced in Eq. (3.29) and Eq. (3.30), for the sums $\hat{S}^{\text{even}}(\Lambda, L)$ and $\hat{S}^{\text{odd}}(\Lambda, L)$ we obtain

$$\hat{S}^{\text{even}}(\Lambda, L) = \frac{\Lambda}{1-\Lambda^2} \\ + \frac{1}{2}(1+L) \coth\left[\frac{1}{2}(1+L)\lambda\right] \cosh(\lambda), \quad \Lambda \geq 1. \quad (C16)$$

and

$$\hat{S}^{\text{even}}(\Lambda, L) = \frac{\Lambda}{1-\Lambda^2} \\ - \frac{1}{2}(1+L) \cot\left[\frac{1}{2}(1+L)\lambda\right] \csc(\lambda), \quad \Lambda \leq 1. \quad (C17)$$

for $\hat{S}^{\text{even}}(\Lambda, L)$, while for the sum $\hat{S}^{\text{odd}}(\Lambda, L)$ one has

$$\hat{S}^{\text{odd}}(\Lambda, L) = \frac{1}{2}(1+L) \frac{\tanh\left[\frac{1}{2}(1+L)\lambda\right]}{\sinh\lambda}, \Lambda \geq 1, \quad (\text{C18})$$

and

$$\hat{S}^{\text{odd}}(\Lambda, L) = \frac{1}{2}(1+L) \frac{\tan\left[\frac{1}{2}(1+L)\lambda\right]}{\sin\lambda}, \Lambda \leq 1. \quad (\text{C19})$$

Obviously, the two pairs Eq. (C16) and Eq. (C17), and Eq. (C18) and Eq. (C19) represent a continuation from real to purely complex values of λ . Because of that, in the remainder we will report only one of the corresponding representations concerning the sums.

From Eq. (C10) and Eq. (C16) one obtains

$$S^{\text{even}}(\Lambda, L) = \frac{L+1}{2} \left\{ \Lambda - \coth\left[\frac{L+1}{2}\lambda\right] \sinh[\lambda] \right\} \quad (\text{C20})$$

whereas from Eq. (C12) and Eq. (C18) one derives

$$S^{\text{odd}}(\Lambda, L) = \frac{L+1}{2} \left\{ \Lambda - \tanh\left[\frac{L+1}{2}\lambda\right] \sinh[\lambda] \right\}. \quad (\text{C21})$$

Using the above expressions and taking into account Eqs. (C2) - (C6) for Δf_h , see Eq. (3.26), one obtains

i) if $p \neq M$ or $q \neq N$:

$$\begin{aligned} -\beta\Delta f_h &= \frac{1}{16K^\perp} \left\{ [h_1^2 + h_L^2 - 2h_L h_1 \cos(\mathbf{k} \cdot \mathbf{\Delta})] \right. \\ &\quad \times \left[\Lambda - \coth\left[\frac{L+1}{2}\lambda\right] \sinh[\lambda] \right] \\ &\quad + [h_1^2 + h_L^2 + 2h_L h_1 \cos(\mathbf{k} \cdot \mathbf{\Delta})] \\ &\quad \times \left[\Lambda - \tanh\left[\frac{L+1}{2}\lambda\right] \sinh[\lambda] \right] \left. \right\}, \quad (\text{C22}) \end{aligned}$$

ii) if $p = M$ and $q = N$

$$\begin{aligned} -\beta\Delta f_h &= \frac{1}{16K^\perp} \left\{ [h_1 - h_L \cos 2\pi(\Delta_x + \Delta_y)]^2 \right. \\ &\quad \times \left[\Lambda - \coth\left[\frac{L+1}{2}\lambda\right] \sinh[\lambda] \right] \\ &\quad + [h_1 + h_L \cos 2\pi(\Delta_x + \Delta_y)]^2 \\ &\quad \times \left[\Lambda - \tanh\left[\frac{L+1}{2}\lambda\right] \sinh[\lambda] \right] \left. \right\}, \quad (\text{C23}) \end{aligned}$$

Note that in deriving the above expression no approximations have been made - it is an *exact* result.

If $L\lambda \gg 1$ from the above one immediately obtains

i) if $p \neq M$ or $q \neq N$:

$$\begin{aligned} -\beta\Delta f_h &\simeq \frac{1}{8K^\perp} \{ \Lambda - \sinh[\lambda] \} \{ h_1^2 + h_L^2 \} \\ &\quad + \frac{1}{2K^\perp} \sinh[\lambda] e^{-(L+1)\lambda} h_1 h_L \cos(\mathbf{k} \cdot \mathbf{\Delta}), \quad (\text{C24}) \end{aligned}$$

and

ii) if $p = M$ and $q = N$

$$\begin{aligned} &-\beta\Delta f_h \simeq \quad (\text{C25}) \\ &\frac{1}{8K^\perp} \{ \Lambda - \sinh[\lambda] \} \{ h_1^2 + \cos 2\pi(\Delta_x + \Delta_y) h_L^2 \} \\ &+ \frac{1}{2K^\perp} \sinh[\lambda] e^{-(L+1)\lambda} h_1 h_L \cos 2\pi(\Delta_x + \Delta_y), \end{aligned}$$

wherefrom one derives the surface part $\Delta f_h^{(s)}$ of the field-dependent term in the free energy

i) if $p \neq M$ or $q \neq N$:

$$-\beta\Delta f_h^{(s)} = \frac{1}{8K^\perp} \{ \Lambda - \sinh[\lambda] \} \{ h_1^2 + h_L^2 \}. \quad (\text{C26})$$

and

ii) if $p = M$ and $q = N$

$$\begin{aligned} -\beta\Delta f_h^{(s)} &= \frac{1}{8K^\perp} \{ \Lambda - \sinh[\lambda] \} \\ &\quad \times \{ h_1^2 + \cos 2\pi(\Delta_x + \Delta_y) h_L^2 \}. \quad (\text{C27}) \end{aligned}$$

From Eqs. (C22) and (C23) one can determine both the transverse and the longitudinal field contribution to the components of the Casimir force. The corresponding results are reported in the main text.

2. Evaluation of the field independent term

We are interested in the L -dependent behavior of the field-independent part of the statistical sum of the system, see Eq. (3.17), where ΔF_0 is given by Eq. (3.11). It is easy to see that

$$\begin{aligned} -\beta\Delta f_0 - \frac{1}{2}L \ln \frac{\pi}{K^\perp} &= -\frac{1}{2} \frac{1}{(2\pi)^2} \int_0^{2\pi} d\theta_1 \int_0^{2\pi} d\theta_2 \quad (\text{C28}) \\ &= -\frac{1}{2} \frac{1}{(2\pi)^2} \int_0^{2\pi} d\theta_1 \int_0^{2\pi} d\theta_2 S_0 \left(\frac{\beta_c}{\beta}, \frac{J^\parallel}{J^\perp}, L \middle| \theta_1, \theta_2 \right) \end{aligned}$$

where

$$\begin{aligned} S_0 \left(\frac{\beta_c}{\beta}, \frac{J^\parallel}{J^\perp}, L \middle| \theta_1, \theta_2 \right) &\equiv \quad (\text{C29}) \\ &\sum_{k=1}^L \ln \left[\frac{s}{K^\perp} - \frac{K^\parallel}{K^\perp} (\cos \theta_1 + \cos \theta_2) - \cos \frac{\pi k}{L+1} \right] \\ &= \sum_{k=1}^L \ln \left[\left(\frac{\beta_c}{\beta} - 1 \right) \left(1 + 2 \frac{J^\parallel}{J^\perp} \right) + \left(1 - \cos \frac{\pi k}{L+1} \right) \right. \\ &\quad \left. + \frac{J^\parallel}{J^\perp} (2 - \cos \theta_1 - \cos \theta_2) \right] \end{aligned}$$

and we have used Eq. (3.6).

The expression in Eq. (C28) can be evaluated in several ways. Let us briefly sketch one of them. By doing so we will also obtain an expression for the free energy that has not been derived before and which are valid not only for large, but for any positive value of L .

Using the identity in Eq. (C14) one can show that

$$S_0 \left(\frac{\beta_c}{\beta}, \frac{J^\parallel}{J^\perp}, L \middle| \theta_1, \theta_2 \right) = -L \ln 2 + \ln \left[\frac{\sinh(1+L)\delta}{\sinh \delta} \right], \quad (\text{C30})$$

where δ is defined in Eq. (3.19). For the contribution of the field-independent term to the transverse Casimir force $\beta \Delta F_{\text{Cas}}^{(0,\perp)}$, see Eq. (3.16), from Eq. (C28) and Eq. (C30) one derives Eq. (3.18) given in the main text. In order to derive the scaling form of $\Delta F_{\text{Cas}}^{(0,\perp)}$ we have to consider the regime $L \gg 1$. Obviously, then Casimir force will be exponentially small if δ is finite. In order to avoid that, one needs $\delta \rightarrow 0$ so that $(L+1)\delta = O(1)$. When δ goes to zero, however, both $(\beta_c/\beta - 1)(1 + 2J^\parallel/J^\perp) \rightarrow 0$ and $\theta_1, \theta_2 \rightarrow 0$. Then, from Eq. (3.19) one obtains

$$\delta^2 = 2 \left(\frac{\beta_c}{\beta} - 1 \right) \left(1 + 2 \frac{J^\parallel}{J^\perp} \right) + \frac{J^\parallel}{J^\perp} (\theta_1^2 + \theta_2^2). \quad (\text{C31})$$

Passing to polar coordinates, from Eq. (3.18) one obtains,

up to exponentially small in L corrections

$$\beta \Delta F_{\text{Cas}}^{(0,\perp)} = -\frac{1}{2} \int_{\delta_{\min}}^{\infty} x^2 [\coth((1+L)x) - 1] \frac{dx}{2\pi} \quad (\text{C32})$$

where

$$\delta_{\min} = \sqrt{2 \left(\frac{\beta_c}{\beta} - 1 \right) \left(1 + 2 \frac{J^\parallel}{J^\perp} \right)}. \quad (\text{C33})$$

Noting that

$$x_t = L\delta_{\min}, \quad (\text{C34})$$

using that

$$\coth x = 1 + 2 \sum_{k=1}^{\infty} e^{-2kx} \quad (\text{C35})$$

and performing the integration in Eq. (C32), one derives Eqs. (3.20) and (3.21) given in the main text. From Eq. (C32) and taking into account the definition (C34) one immediately concludes that $X_{\text{Cas}}^{(0,\perp)}(x_t)$ is a *monotonically increasing* function of x_t .

-
- [1] H. W. Diehl, in *Phase Transitions and Critical Phenomena*, Vol. 10, edited by C. Domb and J. L. Lebowitz (Academic, New York, 1986) p. 76.
 - [2] M. Krech, *Casimir Effect in Critical Systems* (World Scientific, Singapore, 1994).
 - [3] J. G. Brankov, D. M. Dantchev, and N. S. Tonchev, *The Theory of Critical Phenomena in Finite-Size Systems - Scaling and Quantum Effects* (World Scientific, Singapore, 2000).
 - [4] F. Soyka, O. Zvyagolskaya, C. Hertlein, L. Helden, and C. Bechinger, Phys. Rev. Lett. **101**, 208301 (2007).
 - [5] S. Rafaï, D. Bonn, and J. Meunier, Physica A **386**, 31 (2007).
 - [6] C. Hertlein, L. Helden, A. Gambassi, S. Dietrich, and C. Bechinger, Nature **451**, 172 (2008).
 - [7] A. Gambassi, A. Maciolek, C. Hertlein, U. Nellen, L. Helden, C. Bechinger, and S. Dietrich, Phys. Rev. E **80**, 061143 (2009).
 - [8] U. Nellen, L. Helden, and C. Bechinger, EPL **88**, 26001 (2009).
 - [9] U. Nellen, J. Dietrich, L. Helden, S. Chodankar, K. Nygrd, J. F. van der Veen, and C. Bechinger, Soft Matter (2011), DOI: 10.1039/C1SM05103B.
 - [10] O. Zvyagolskaya, A. J. Archer, and C. Bechinger, EPL **96**, 28005 (2011).
 - [11] P. Nowakowski and M. Napiórkowski, Phys. Rev. E **78**, 060602 (2008).
 - [12] P. Nowakowski and M. Napiórkowski, J. Phys. A: Math. Gen. **42**, 475005 (2009).
 - [13] D. B. Abraham and A. Maciolek, Phys. Rev. Lett. **105**, 055701 (2010).
 - [14] P. Nowakowski and M. Napirkowski, The Journal of Chemical Physics **141**, 064704 (2014), <http://dx.doi.org/10.1063/1.4892343>.
 - [15] Z. Borjan, Phys. Rev. E **91**, 032121 (2015).
 - [16] Z. Borjan, EPL (Europhysics Letters) **99**, 56004 (2012).
 - [17] Maciolek, A. A., Ciach, and A. Drzewiński, pre **60**, 2887 (1999).
 - [18] A. Drzewiński, A. Maciolek, and A. Ciach, Phys. Rev. E **61**, 5009 (2000).
 - [19] A. Drzewiński, A. Maciolek, and R. Evans, Phys. Rev. Lett. **85**, 3079 (2000).
 - [20] M. Zubaszewska, A. Maciolek, and A. Drzewiński, Phys. Rev. E **88**, 052129 (2013).
 - [21] O. A. Vasilyev, E. Eisenriegler, and S. Dietrich, Phys. Rev. E **88**, 012137 (2013).
 - [22] J. Dubail, R. Santachiara, and T. Emig, EPL (Europhysics Letters) **112**, 66004 (2015).
 - [23] X. Wu and N. Izmailyan, Phys. Rev. E **91**, 012102 (2015).
 - [24] O. Vasilyev, A. Gambassi, A. Maciolek, and S. Dietrich, Phys. Rev. E **79**, 041142 (2009).
 - [25] M. Hasenbusch, Phys. Rev. B **83**, 134425 (2011).
 - [26] O. Vasilyev, A. Maciolek, and S. Dietrich, Phys. Rev. E **84**, 041605 (2011).
 - [27] F. Parisen Toldin, M. Tröndle, and S. Dietrich, Phys. Rev. E **88**, 052110 (2013).
 - [28] O. A. Vasilyev and S. Dietrich, EPL (Europhysics Letters) **104**, 60002 (2013).
 - [29] O. A. Vasilyev, Phys. Rev. E **90**, 012138 (2014).
 - [30] A. Maciolek, O. Vasilyev, V. Dotsenko, and S. Dietrich, Phys. Rev. E **91**, 032408 (2015).
 - [31] G. Palágyi and S. Dietrich, Phys. Rev. E **70**, 046114 (2004).
 - [32] M. Krech, Phys. Rev. E **56**, 1642 (1997).
 - [33] T. F. Mohry, A. Maciolek, and S. Dietrich, Phys. Rev. E **81**, 061117 (2010).

- [34] G. Valchev, D. Dantchev, and K. Kostadinov, *IJIMR* **2**, 152012 (2012).
- [35] M. Tröndle, L. Harnau, and S. Dietrich, *Journal of Physics: Condensed Matter* **27**, 214006 (2015).
- [36] G. Valchev and D. Dantchev, *Phys. Rev. E* **92**, 012119 (2015).
- [37] R. Okamoto and A. Onuki, *The Journal of Chemical Physics* **136**, 114704 (2012).
- [38] V. Privman, “Finite size scaling and numerical simulations of statistical systems,” (World Scientific, Singapore, 1990) Chap. Finite-size scaling theory, p. 1.
- [39] A. Ajdari, L. Peliti, and J. Prost, *Phys. Rev. Lett.* **66**, 1481 (1991).
- [40] H. Li and M. Kardar, *Phys. Rev. A* **46**, 6490 (1992).
- [41] P. Zihlerl, R. Podgornik, and S. Žumer, *Chem. Phys. Lett.* **295**, 99 (1998).
- [42] M. Kardar and R. Golestanian, *Rev. Mod. Phys.* **71**, 1233 (1999).
- [43] D. Bartolo, D. Long, and J.-B. Fournier, *Europhys. Lett.* **49**, 729 (2000).
- [44] R. Golestanian, A. Ajdari, and J.-B. Fournier, *Phys. Rev. E* **64**, 022701 (2001).
- [45] F. K. P. Haddadan, F. Schlesener, and S. Dietrich, *Phys. Rev. E* **70**, 041701 (2004).
- [46] F. Karimi Pour Haddadan, A. Naji, A. K. Seifi, and R. Podgornik, *J. Phys.: Condens. Matter* **26**, 075103 (2014), arXiv:1310.8501 [cond-mat.soft].
- [47] F. K. P. Haddadan, A. Naji, N. Shirzadiani, and R. Podgornik, *Journal of Physics: Condensed Matter* **26**, 505101 (2014).
- [48] J. O. Indekeu, *J. Chem. Soc. Faraday Trans. II* **82**, 1835 (1986).
- [49] R. Garcia and M. H. W. Chan, *Phys. Rev. Lett.* **83**, 1187 (1999).
- [50] R. Garcia and M. H. W. Chan, *Phys. Rev. Lett.* **88**, 086101 (2002).
- [51] R. Zandi, J. Rudnick, and M. Kardar, *Phys. Rev. Lett.* **93**, 155302 (2004).
- [52] A. Ganshin, S. Scheidemantel, R. Garcia, and M. H. W. Chan, *Phys. Rev. Lett.* **97**, 075301 (2006).
- [53] A. Maciòlek, A. Gambassi, and S. Dietrich, *Phys. Rev. E* **76**, 031124 (2007).
- [54] T. Ueno, S. Balibar, T. Mizusaki, F. Caupin, and E. Rolley, *Phys. Rev. Lett.* **90**, 116102 (2003).
- [55] J. Bergknoff, D. Dantchev, and J. Rudnick, *Phys. Rev. E* **84**, 041134 (2011).
- [56] N. D. Mermin and H. Wagner, *Phys. Rev. Lett.* **17**, 1133 (1966).
- [57] M. E. Fisher, *Am. J. Phys.* **32**, 343 (1964).
- [58] G. S. Joyce, *Phys. Rev. Lett.* **19**, 581 (1967).
- [59] G. S. Joyce, *Phys. Rev.* **155**, 478 (1967).
- [60] H. E. Stanley, *Phys. Rev.* **176**, 718 (1968).
- [61] R. K. Pathria and P. D. Beale, *Statistical Mechanics*, 3rd ed. (Elsevier, 2011).
- [62] S. Singh and R. K. Pathria, *Phys. Rev. B* **31**, 4483 (1985).
- [63] G. W. Gray and S. M. Kelly, *Journal of Materials Chemistry* **9**, 2037 (1999).
- [64] R. P. Feynman in C. J. Gorter, ed., *Progress in low temperature physics*, Series in physics, Vol. 1 (North-Holland Pub. Co.; sole distributors for U.S.A.: Interscience Publishers, Amsterdam, New York, 1955) pp. 17–53.
- [65] V. L. Ginzburg and L. P. Pitaevskii, *Soviet Physics JETP* **7**, 858 (1958).
- [66] M. Abramowitz and I. A. Stegun, *Handbook of mathematical functions with formulas, graphs, and mathematical tables* (Dover Publications, New York, 1970).
- [67] F. W. J. Olver, D. W. Lozier, R. F. Boisvert, and C. W. C. (editors), *NIST Handbook of Mathematical Functions* (NIST and Cambridge University Press, 2010).
- [68] I. S. Gradshteyn and I. H. Ryzhik, *Table of Integrals, Series, and Products*, edited by A. Jeffrey and D. Zwillinger (Academic, New York, 2007).